

Topological contribution to magnetism in the Kane-Mele model: An explicit wave function approach

Soshun Ozaki^{1,*} and Masao Ogata^{1,2}

¹*Department of Physics, University of Tokyo, Bunkyo, Tokyo 113-0033, Japan*

²*Trans-scale Quantum Science Institute, University of Tokyo, Bunkyo, Tokyo 113-0033, Japan*

(Dated: April 22, 2022)

In our previous publication [S. Ozaki and M. Ogata, Phys. Rev. Research **3**, 013058], the quantization of the orbital-Zeeman (OZ) cross term in the magnetic susceptibility, or the cross term of spin Zeeman and orbital effect, was shown for the Kane-Mele model using the expansion around the Dirac points. In the present study, we accurately evaluate the orbital, spin-Zeeman, and OZ cross term of the Kane-Mele model using a recently developed formulation. This formula is written in terms of the explicit Bloch wave functions, and enables us to evaluate each contribution taking account of the integration over the whole Brillouin zone and the summation over all the bands. As a result, additional contributions such as core-electron diamagnetism are found. Furthermore, our evaluation confirms the quantization of the OZ cross term and reveals its behavior including the metallic case. The possibility of experimental detection of the quantization is discussed.

I. INTRODUCTION

Much research in recent years has focused on topological insulators (TIs). [1–14] TIs show anomalous phenomena such as electric conduction on sample surfaces, and the search for candidate materials is one of the most important problems in this field. In particular, the novel phenomena such as spin Hall effect and the conducting edge state robust against nonmagnetic impurities are expected in two-dimensional (2D) TIs. However, only a few materials have been confirmed to be 2D TIs. [8–12] So far, the confirmation of TI is achieved by finding the edge state in angle-resolved photoemission spectroscopy and in the transport experiments, which are both by the methods to find the anomalous edge states. Therefore, it is desirable to develop some alternative methods that detect the topological nature of a material through some observation of bulk physical quantities. One example for such quantities is the magnetic susceptibility.

Usually, the magnetic susceptibility in itinerant systems without two-body interactions is discussed in terms of the spin Zeeman effect and the orbital effect individually. Generally, however, in the system with spin-orbit interaction (SOI) the cross term of the two exists, which we call “orbital-Zeeman (OZ) cross term” in the following. Although the OZ cross term were discussed for some situations [7, 15–21], further research on it is desired.

Nakai and Nomura [15] reported that the OZ cross term χ_{OZ} in the Bernevig-Hughes-Zhang model [5] is proportional to the spin Chern number $Ch_{s,l}$, the topological invariant for spin-conserving 2D TIs. Recently, we clarified that the coefficient of $Ch_{s,l}$ is generally given by the universal value $\chi_u = 4|e|\mu_B/h$, and confirmed the quantization in the Kane-Mele model [2, 3] by using the $\mathbf{k} \cdot \mathbf{p}$ approximation explicitly [21]. This quantization is associated with the Berry curvature, and physically, it origi-

ates from the edge currents characteristic of the 2D TIs [21]. Based on these results, the magnetic susceptibility is expected to be used for the detection of the change in the topological invariant for 2D TIs. However, the evaluation for the Kane-Mele model in the previous paper was based on the effective Hamiltonian in the vicinities of K and K' points of graphene, where the massless Dirac electron system is realized. Therefore, the contributions from the distant \mathbf{k} region from the K or K' points or from the bands other than the two bands forming the Dirac dispersion were not evaluated precisely. Besides, the previous publication does not include some additional contributions, such as core-electron diamagnetism, the newly found Fermi surface term, and the correction term from the occupied states [22–24]. To compare the theory with experiments, it is desirable to be able to evaluate all these contributions.

Therefore, in this paper, we clarify all the contributions in magnetic susceptibility including the spin Zeeman, orbital, and OZ cross term in the Kane-Mele model, taking care of the contributions from the whole Brillouin zone. We will show that the OZ cross term has a reasonable magnitude compared with the other contributions and confirm the quantized jump at the topological phase transition. We also study the chemical potential dependence of each contribution and find that the OZ cross term also has a contribution at the van Hove singularity irrespective of whether the system is topological or not.

Here, it should be noted that the Kane-Mele model is based on the tight-binding model of graphene. The effect of the magnetic field is often introduced as the Peierls phase of the transfer integral in the tight-binding model. However, it is known that the Peierls phase is not enough to describe the effect of the magnetic field [25, 26]. To obtain the whole magnetic susceptibility, it is necessary to use the continuum Hamiltonian with the SOI. The formulation of the orbital magnetism in such a case is not so simple owing to the complicated inter-band effects of the magnetic field, and a lot of efforts

* ozaki@hosi.phys.s.u-tokyo.ac.jp

were dedicated [27–33]. It is notable that Fukuyama developed a one-line formula for the orbital magnetic susceptibility, which is written in terms of Green's functions [33]. (Some recent publications [34, 35] proposed similar formulae.) Fukuyama's formula was reformulated in terms of Bloch wave functions with infinite summations over the band indices taken analytically [22, 36], and the resultant formula properly includes the Landau-Peierls (dia)magnetism and the contribution from occupied states, and some additional contributions. The total magnetic susceptibility is given by

$$\chi_{\text{total}} = \chi_{\text{LP}} + \chi_{\text{inter}} + \chi_{\text{FS}} + \chi_{\text{FS-P}} + \chi_{\text{occ1}} + \chi_{\text{occ2}}, \quad (1)$$

where χ_{LP} , χ_{inter} , χ_{FS} , and χ_{occ1} represent Landau-Peierls, interband, Fermi surface, and occupied state contributions, respectively. $\chi_{\text{FS-P}}$ is also the Fermi surface contribution, which contains Pauli paramagnetism. χ_{occ2} is a Berry curvature-related term. The explicit expressions for these contributions are shown in Ref. [36]. To apply the above formula to the tight-binding model of Kane-Mele, we use the method of linear combination of atomic orbitals (LCAOs) for the p_z orbitals on carbon atoms as in the case of simple graphene [24]. Then, we evaluate Eq. (1) using the obtained wave functions and study various contributions in the orbital term, spin Zeeman term, and OZ cross term.

This paper is organized as follows. In Sec. II, we first review the fundamental properties of the Kane-Mele model such as the energy dispersion and topological phase diagram. Then, we derive the continuum-space Bloch wave function assuming that it consists of $2p_z$ atomic orbitals. In Sec. III, we apply the general formula for the magnetic susceptibility to the Kane-Mele model and derive analytic expressions for each contribution. In Sec. IV, we numerically evaluate the results obtained in the previous section and discuss the experimental observability of each term, especially the OZ cross term. Section V is devoted to summary.

II. EXPLICIT WAVE FUNCTIONS FOR THE KANE-MELE MODEL

We study the energy dispersion and write down the explicit wave functions for the Kane-Mele model. The tight-binding Hamiltonian is given by [2, 3]

$$H = - \sum_{\langle i,j \rangle \alpha} t c_{i\alpha}^\dagger c_{j\alpha} + \Delta_0 \left(\sum_{i \in A, \alpha} c_{i\alpha}^\dagger c_{i\alpha} - \sum_{i \in B, \alpha} c_{i\alpha}^\dagger c_{i\alpha} \right) + \sum_{\langle\langle i,j \rangle\rangle, \alpha, \beta} it_2 \nu_{ij} c_{i\alpha}^\dagger \sigma_{\alpha\beta}^z c_{j\beta}, \quad (2)$$

where $c_{i\alpha}^\dagger$ creates an electron with spin α at site i , and $\langle i, j \rangle$ ($\langle\langle i, j \rangle\rangle$) run over all the nearest- (next-nearest-) neighbor sites of a two-dimensional honeycomb lattice

defined in Fig. 1. The first term represents usual nearest-neighbor hoppings with transfer integral t . The second term represents a staggered on-site potential, $+\Delta_0$ for the sites in the A sublattice and $-\Delta_0$ for those in the B sublattice. The summation $\sum_{i \in A}$ ($\sum_{i \in B}$) means the sum over the sites in the A (B) sublattice. The last term represents the hopping between the next-nearest-neighbor sites due to SOI, where $\sigma_{\alpha\beta}^z$ is the $(\alpha\beta)$ component of the spin operator in the z direction, and $\nu_{ij} = -\nu_{ji} = +1$ (-1) if the electron makes a left (right) turn to propagate to a next-nearest site [see Fig. 1]. Only the σ^z component of SOI appears, [3, 37, 38] whose microscopic derivation using the LACOs is shown in Appendix A. This model is known as the model for silicene [37–41], in which we can control Δ_0 by changing the electric field applied perpendicularly to the layer owing to the buckled structure of silicene.

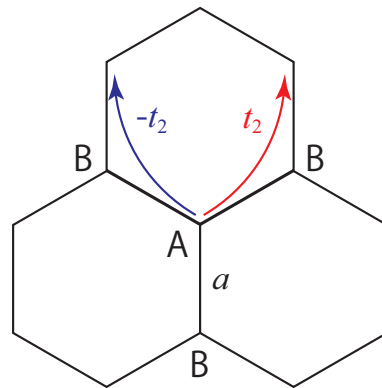


FIG. 1. Honeycomb lattice for the Kane-Mele model. A and B represent the sublattices and a is the distance between adjacent two sites. The arrows show the hopping between the next-nearest-neighbors due to SOI. The signs of this hopping depends on the path: It is $+1$ (-1) if the electron makes a left (right) turn to propagate to a next-nearest site.

As discussed in Sec. I, to include all the effect of a magnetic field correctly, we consider the Hamiltonian in the continuum space,

$$H^{\text{full}} = \frac{1}{2m}(\mathbf{p} - e\mathbf{A})^2 + V(\mathbf{r}) + \frac{\hbar^2}{8m^2c^2}\nabla^2V + \frac{\hbar}{4m^2c^2}\boldsymbol{\sigma} \cdot \nabla V \times (\mathbf{p} - e\mathbf{A}) - \frac{e\hbar}{2m}\boldsymbol{\sigma} \cdot \mathbf{B}, \quad (3)$$

where e (< 0) is the electron charge, $\mathbf{A}(\mathbf{r})$ is a vector potential ($\mathbf{B} = \text{rot}\mathbf{A}$). $V(\mathbf{r})$ is the periodic potential that represents the honeycomb lattice and the fourth term represents the SOI derived from the relativistic Dirac equation. We have set the g factor in the last term (spin Zeeman term) to be $g = 2$ neglecting the QED corrections. When we consider a tight-binding model under a magnetic field, a renormalization of the g factor generally occurs owing to the virtual interband process [42, 43], and the effective g factor deviates from $g = 2$ in the focused bands. However, since the Hamiltonian Eq. (3) contains all the bands, the Zeeman term in Eq. (3) should have

the bare g factor, $g = 2$. At the end of calculation including the interband processes, the effective g factor should naturally appear.

We apply Eq. (3) to the Kane-Mele model. In Eq. (3), $V(\mathbf{r})$ is chosen to be the periodic potential formed by the atoms on the honeycomb lattice,

$$V(\mathbf{r}) = \sum_{i \in \text{A}} V_{\text{A}}(\mathbf{r} - \mathbf{R}_{\text{Ai}}) + \sum_{i \in \text{B}} V_{\text{B}}(\mathbf{r} - \mathbf{R}_{\text{Bi}}), \quad (4)$$

where \mathbf{R}_{Ai} (\mathbf{R}_{Bi}) represents the position of the site in the A (B) sublattice in the i th unit cell. For the continuum Hamiltonian Eq. (3), we write down the Bloch wave functions in terms of LCAOs of the A and B sublattice [24], assuming that the wave functions near the Fermi level consist of $2p_z$ orbitals. Then, the wave functions are expressed as the linear combinations of the orthogonal wave functions localized at a site $\mathbf{r} = \mathbf{R}_i$. (The other bands are treated later.) Using the wave function for $2p_z$ orbital,

$$\phi_{2p_z}(\mathbf{r}) = \frac{1}{\sqrt{24}(a_{\text{B}}^*)^{5/2}} \sqrt{\frac{3}{4\pi}} z e^{-r/2a_{\text{B}}^*} \quad (5)$$

with a_{B}^* being the renormalized Bohr radius, the orthogonal localized basis is given by [23–25]

$$\Phi(\mathbf{r} - \mathbf{R}_i) = \phi_{2p_z}(\mathbf{r} - \mathbf{R}_i) - \sum_{j:\text{n.n.}} \frac{s}{2} \phi_{2p_z}(\mathbf{r} - \mathbf{R}_j). \quad (6)$$

Here, the renormalized Bohr radius is $a_{\text{B}}^* = a_{\text{B}}/Z_{\text{eff}}$, where $a_{\text{B}} = \hbar^2/m_e e^2$ is the Bohr radius and $Z_{\text{eff}} = 3.25$ [24, 44] is the effective charge of carbon atoms. In Eq. (6), j summation is taken over the nearest-neighbor (n.n.) sites of \mathbf{R}_i , and s is the overlap integral between the adjacent sites,

$$s = \int \phi_{2p_z}^*(\mathbf{r} - \mathbf{R}_i) \phi_{2p_z}(\mathbf{r} - \mathbf{R}_j) d\mathbf{r}. \quad (7)$$

The orthogonality of $\Phi(\mathbf{r} - \mathbf{R}_i)$ is maintained up to the first order with respect to s . Note that s is independent of the direction $\mathbf{R} = \mathbf{R}_j - \mathbf{R}_i$ since the p_z orbital is isotropic in the xy -plane.

Next, we perform a Fourier transform and obtain the basis

$$\varphi_{\text{A}\mathbf{k}}(\mathbf{r}) = \frac{1}{\sqrt{N}} \sum_{\mathbf{R}_{\text{Ai}}} e^{-i\mathbf{k}(\mathbf{r} - \mathbf{R}_{\text{Ai}})} \Phi(\mathbf{r} - \mathbf{R}_{\text{Ai}}), \quad (8)$$

and

$$\varphi_{\text{B}\mathbf{k}}(\mathbf{r}) = \frac{1}{\sqrt{N}} \sum_{\mathbf{R}_{\text{Bi}}} e^{-i\mathbf{k}(\mathbf{r} - \mathbf{R}_{\text{Bi}})} \Phi(\mathbf{r} - \mathbf{R}_{\text{Bi}}), \quad (9)$$

where N is the total number of sites on each sublattice. The periodic part of the Bloch wave function $u_{l\mathbf{k}\sigma}(\mathbf{r})$ is determined by the eigenvalue equation,

$$H_{\mathbf{k}\sigma} u_{l\mathbf{k}\sigma} = E_{l\mathbf{k}\sigma} u_{l\mathbf{k}\sigma}, \quad H_{\mathbf{k}\sigma} = e^{-i\mathbf{k}\mathbf{r}} H^{\text{full}} e^{i\mathbf{k}\mathbf{r}}, \quad (10)$$

where l and $\sigma (= \pm 1)$ represent the band index and the eigenvalue of the z -component of spin of an electron: $\sigma = 1$ for spin-up and $\sigma = -1$ for spin-down. We denote the two energy dispersion and the two eigenfunctions near the Fermi level as $E_{\mathbf{k}\sigma}^{\pm}$ and $u_{\mathbf{k}\sigma}^{\pm}(\mathbf{r})$, respectively. To determine $E_{\mathbf{k}\sigma}^{\pm}$ and $u_{\mathbf{k}\sigma}^{\pm}(\mathbf{r})$, we calculate the matrix elements of the Hamiltonian $H_{\mathbf{k}\sigma}$ in terms of the obtained basis,

$$h_{nm\sigma}(\mathbf{k}) = \int \varphi_{n\mathbf{k}}^*(\mathbf{r}) H_{\mathbf{k}\sigma} \varphi_{m\mathbf{k}}(\mathbf{r}) d\mathbf{r}, \quad (11)$$

with $n, m = \text{A}, \text{B}$. They become

$$h_{\text{AA}\sigma} = \Delta_{\mathbf{k}\sigma} + E_0, \quad (12)$$

$$h_{\text{BB}\sigma} = -\Delta_{\mathbf{k}\sigma} + E_0, \quad (13)$$

$$h_{\text{AB}\sigma} = h_{\text{BA}\sigma}^* = -t\gamma_{\mathbf{k}}, \quad (14)$$

where E_0 is the energy constant [24],

$$\Delta_{\mathbf{k}\sigma} = \Delta_0 + 4\sigma t_2 \sin \frac{\sqrt{3}}{2} k_x a \left(\cos \frac{3}{2} k_y a - \cos \frac{\sqrt{3}}{2} k_x a \right), \quad (15)$$

and,

$$\gamma_{\mathbf{k}} = e^{-ik_y a} + e^{i(\frac{\sqrt{3}}{2} k_x + \frac{1}{2} k_y) a} + e^{i(-\frac{\sqrt{3}}{2} k_x + \frac{1}{2} k_y) a}, \quad (16)$$

with a being the distance between the nearest-neighbor sites. Hereafter, we set $E_0 = 0$ without loss of generality. Δ_0 corresponds to the staggered on-site potential in Eq. (2) and the nearest-neighbor hopping t can be expressed as a kind of overlap integral [24]. As shown in Appendix A, the SOI in Eq. (3) does not give contributions to the nearest-neighbor hopping, but it leads to a next-nearest-neighbor hopping t_2 in Eq. (2), which is also expressed by a kind of the overlap integrals. In Appendix A, it is also shown that the next-nearest-neighbor hopping have only the z component of spin $\sigma_{\sigma\sigma}^z$; therefore, the spin is conserved.

By diagonalizing the Hamiltonian $h_{nm\sigma}(\mathbf{k})$, we obtain the energy dispersion,

$$E_{\mathbf{k}\sigma}^{\pm} = \pm \sqrt{\Delta_{\mathbf{k}\sigma}^2 + \varepsilon_{\mathbf{k}}^2}, \quad (17)$$

where $\varepsilon_{\mathbf{k}} := t|\gamma_{\mathbf{k}}|$. At $\text{K} = (4\pi/3\sqrt{3}a, 0)$ and $\text{K}' = (-4\pi/3\sqrt{3}a, 0)$ in the Brillouin zone, $\gamma_{\mathbf{k}}$ vanishes. Figure 2 shows the energy dispersions Eq. (17) with $\sigma = +1$ (up spin)[21]. The solid and the dashed lines in Fig. 2 are for the cases of $\Delta_0/t = 1/4$, $t_2/t = \sqrt{3}/72$ (topologically trivial) and $\Delta_0/t = 1/4$, $t_2/t = \sqrt{3}/24$ (topologically nontrivial), respectively. The dispersions are similar to those of graphene but gaps open at K and K' points. The magnitudes of the gaps at K and K' points are given by

$$2 \left| \Delta_0 + 3\sqrt{3}\sigma t_2 \right|, \quad 2 \left| \Delta_0 - 3\sqrt{3}\sigma t_2 \right|, \quad (18)$$

respectively. Owing to the SOI, the energy dispersions

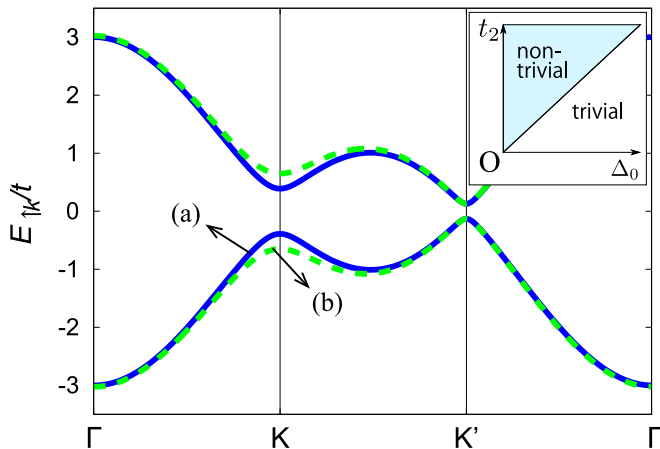


FIG. 2. Energy dispersion of Eq. (2) for $\sigma = 1$ (up spin) along the path $\Gamma \rightarrow K \rightarrow K' \rightarrow \Gamma$ for two typical choices of parameters: (a) solid line, $\Delta_0/t = 1/4$, $t_2/t = \sqrt{3}/72$ (topologically trivial) and (b) dashed line, $\Delta_0/t = 1/4$, $t_2/t = \sqrt{3}/24$ (topologically nontrivial). The energy dispersion for $\sigma = -1$ (down spin) is obtained by exchanging K for K' points. Inset: Phase diagram of the present model. This figure is taken from Ref.[21].

for spin-up and spin-down are not the same. The energy dispersion for $\sigma = -1$ (down spin) is obtained by exchanging K for K' points in Fig. 2. As shown in the inset of Fig. 2 [2, 3, 37, 38], the system is topologically trivial for $|\Delta_0| > 3\sqrt{3}|t_2|$ while the system is topologically nontrivial for $|\Delta_0| < 3\sqrt{3}|t_2|$. As usual, the gap closes at the nontrivial-trivial critical points, $\Delta_0 = \pm 3\sqrt{3}t_2$.

The two eigenfunctions, $u_{l\sigma k\sigma}^\pm(\mathbf{r})$, are obtained as

$$u_{k\sigma}^+(\mathbf{r}) = e^{\frac{i}{2}\theta_{\mathbf{k}}} \cos \eta_{k\sigma} \varphi_{A\mathbf{k}}(\mathbf{r}) - e^{-\frac{i}{2}\theta_{\mathbf{k}}} \sin \eta_{k\sigma} \varphi_{B\mathbf{k}}(\mathbf{r}), \quad (19)$$

and

$$u_{k\sigma}^-(\mathbf{r}) = e^{\frac{i}{2}\theta_{\mathbf{k}}} \sin \eta_{k\sigma} \varphi_{A\mathbf{k}}(\mathbf{r}) + e^{-\frac{i}{2}\theta_{\mathbf{k}}} \cos \eta_{k\sigma} \varphi_{B\mathbf{k}}(\mathbf{r}), \quad (20)$$

where

$$e^{i\theta_{\mathbf{k}}} = \frac{\gamma_{\mathbf{k}}}{|\gamma_{\mathbf{k}}|}, \quad (21)$$

$$\cos \eta_{k\sigma} = \sqrt{\frac{1}{2} \left(1 + \frac{\Delta_{k\sigma}}{|E_{k\sigma}^\pm|} \right)}, \quad (22)$$

$$\sin \eta_{k\sigma} = \sqrt{\frac{1}{2} \left(1 - \frac{\Delta_{k\sigma}}{|E_{k\sigma}^\pm|} \right)}. \quad (23)$$

If we set $\eta_{k\sigma} = \frac{\pi}{4}$, these eigenfunctions coincide with those for (massless) graphene [24].

Note that the Hamiltonian Eq. (3) contains all the bands. In the following, the eigenenergies and eigenfunctions of all the other bands are denoted as $E_{l'\mathbf{k}\sigma}$ and $u_{l'\mathbf{k}\sigma}(\mathbf{r})$ with $l' \neq \pm$. As we will show later, they are used in the interband contribution of magnetic susceptibility χ_{inter} , but the explicit forms of $E_{l'\mathbf{k}\sigma}$ and $u_{l'\mathbf{k}\sigma}(\mathbf{r})$ are not necessary.

III. MAGNETIC SUSCEPTIBILITY

Generally, the magnetic susceptibility consists of six contributions shown in Eq. (1)[22, 36]. Using the eigenenergies and eigenfunctions mentioned above, each term in Eq. (1) becomes

$$\chi_{\text{LP}} = \frac{e^2}{12\hbar^2} \sum_{\pm, \mathbf{k}\sigma} f'(E_{\mathbf{k}\sigma}^{\pm}) \left[\frac{\partial^2 E_{\mathbf{k}\sigma}^{\pm}}{\partial k_x^2} \frac{\partial^2 E_{\mathbf{k}\sigma}^{\pm}}{\partial k_y^2} - \left(\frac{\partial^2 E_{\mathbf{k}\sigma}^{\pm}}{\partial k_x \partial k_y} \right)^2 \right] \quad (24)$$

$$\chi_{\text{inter}} = -2 \sum_{\pm} \sum_{l' \neq \pm, \mp} \sum_{\mathbf{k}, \sigma} \frac{f(E_{\mathbf{k}\sigma}^{\pm})}{E_{\mathbf{k}\sigma}^{\pm} - E_{l'\mathbf{k}\sigma}} |M_{\pm l'\sigma}|^2 \quad (25)$$

$$\begin{aligned} \chi_{\text{FS}} = & \frac{e^2}{2\hbar^2} \text{Re} \sum_{\pm, \mathbf{k}, \sigma} f'(E_{\mathbf{k}\sigma}^{\pm}) \left[\left\{ \frac{\partial E_{\mathbf{k}\sigma}^{\pm}}{\partial k_x} \int \frac{\partial u_{\mathbf{k}\sigma}^{\pm*}}{\partial k_y} \left(\frac{\partial H_{\mathbf{k}}}{\partial k_x} + \frac{\partial E_{\mathbf{k}\sigma}^{\pm}}{\partial k_x} \right) \frac{\partial u_{\mathbf{k}\sigma}^{\pm}}{\partial k_y} d\mathbf{r} \right. \right. \\ & \left. \left. - \frac{\partial E_{\mathbf{k}\sigma}^{\pm}}{\partial k_x} \int \frac{\partial u_{\mathbf{k}\sigma}^{\pm*}}{\partial k_x} \left(\frac{\partial H_{\mathbf{k}}}{\partial k_y} + \frac{\partial E_{\mathbf{k}\sigma}^{\pm}}{\partial k_y} \right) \frac{\partial u_{\mathbf{k}\sigma}^{\pm}}{\partial k_y} d\mathbf{r} + (x \leftrightarrow y) \right\} - \left\{ \frac{\hbar^2}{m} \frac{\partial E_{\mathbf{k}\sigma}^{\pm}}{\partial k_x} \int u_{\mathbf{k}\sigma}^{\pm*} \sigma_z \frac{\partial u_{\mathbf{k}\sigma}^{\pm}}{\partial k_y} d\mathbf{r} - (x \leftrightarrow y) \right\} \right] \quad (26) \end{aligned}$$

$$\chi_{\text{FS-P}} = - \sum_{\pm, \mathbf{k}, \sigma} f'(E_{\mathbf{k}\sigma}^{\pm}) |M_{\pm \pm \sigma}|^2 \quad (27)$$

$$\chi_{\text{occ1}} = -\frac{e^2}{4\hbar^2} \sum_{\pm, \mathbf{k}, \sigma} f(E_{\mathbf{k}\sigma}^{\pm}) \left[\frac{\partial^2 E_{\mathbf{k}\sigma}^{\pm}}{\partial k_x \partial k_y} \int \frac{\partial u_{\mathbf{k}\sigma}^{\pm*}}{\partial k_x} \frac{\partial u_{\mathbf{k}\sigma}^{\pm}}{\partial k_y} d\mathbf{r} + \left(\frac{\hbar^2}{m} - \frac{\partial^2 E_{\mathbf{k}\sigma}^{\pm}}{\partial k_x^2} \right) \int \frac{\partial u_{\mathbf{k}\sigma}^{\pm*}}{\partial k_y} \frac{\partial u_{\mathbf{k}\sigma}^{\pm}}{\partial k_y} d\mathbf{r} \right] + (x \leftrightarrow y) \quad (28)$$

$$\chi_{\text{occ2}} = -\frac{e}{\hbar} \text{Re} \sum_{\pm, \mathbf{k}, \sigma} f(E_{\mathbf{k}\sigma}^{\pm}) M_{\pm \pm \sigma} \Omega_{\pm \sigma}, \quad (29)$$

where $M_{ll'\sigma}$ is the magnetic moment defined by

$$\begin{aligned} M_{ll'\sigma} = & -\frac{ie}{2\hbar} \left\{ \int \frac{\partial u_{l\mathbf{k}\sigma}^*}{\partial k_x} \left(\frac{\partial H_{\mathbf{k}}}{\partial k_y} + \frac{\partial E_{l\mathbf{k}\sigma}}{\partial k_y} \right) u_{l'\mathbf{k}\sigma} d\mathbf{r} \right. \\ & \left. - \int \frac{\partial u_{l\mathbf{k}\sigma}^*}{\partial k_y} \left(\frac{\partial H_{\mathbf{k}}}{\partial k_x} + \frac{\partial E_{l\mathbf{k}\sigma}}{\partial k_x} \right) u_{l'\mathbf{k}\sigma} d\mathbf{r} \right\} \\ & + \frac{e\hbar}{2m} \int u_{l\mathbf{k}\sigma}^* \sigma_z u_{l'\mathbf{k}\sigma} d\mathbf{r}, \quad (30) \end{aligned}$$

and $\Omega_{\pm\sigma}$ is the z -component of the Berry curvature

$$\Omega_{\pm\sigma} = i \int d\mathbf{r} \left(\frac{\partial u_{\mathbf{k}\sigma}^{\pm*}}{\partial k_x} \frac{\partial u_{\mathbf{k}\sigma}^{\pm}}{\partial k_y} - \frac{\partial u_{\mathbf{k}\sigma}^{\pm*}}{\partial k_y} \frac{\partial u_{\mathbf{k}\sigma}^{\pm}}{\partial k_x} \right). \quad (31)$$

In principle, there are contributions of core level electrons (i.e., in the $1s$ orbital etc.) in χ_{occ1} and χ_{occ2} , which we do not consider in the following.

Various integrals appearing in the above equations are calculated by using the Bloch wave functions in Eqs. (19) and (20) up to the first order with respect to the ‘‘overlap integrals’’ s , t , and t_2 , whose integrands contain the overlap of atomic orbitals $\phi_{2p_z}^*(\mathbf{r} - \mathbf{R}_j) \phi_{2p_z}(\mathbf{r} - \mathbf{R}_i)$ with \mathbf{R}_i and \mathbf{R}_j being the nearest-neighbor sites or next-nearest-neighbor sites. The obtained integrals are shown in Appendix B. In the following, we write $E_{\mathbf{k}\sigma} := \sqrt{\Delta_{\mathbf{k}\sigma}^2 + \varepsilon_{\mathbf{k}}^2}$ (i.e., $E_{\mathbf{k}\sigma}^{\pm} = \pm E_{\mathbf{k}\sigma}$). Furthermore, to simplify the expressions we abbreviate $\varepsilon_{\mathbf{k}}$, $\theta_{\mathbf{k}}$, $E_{\mathbf{k}\sigma}$, $\Delta_{\mathbf{k}\sigma}$, and $\eta_{\mathbf{k}\sigma}$ as ε , θ , E , Δ , and η , respectively, as far as they do not cause

ambiguity. We also use the abbreviations,

$$\begin{aligned} \varepsilon_{\mu} &= \frac{\partial \varepsilon}{\partial k_{\mu}}, & \theta_{\mu} &= \frac{\partial \theta}{\partial k_{\mu}}, & E_{\mu} &= \frac{\partial E}{\partial k_{\mu}}, & \Delta_{\mu} &= \frac{\partial \Delta}{\partial k_{\mu}}, \\ \eta_{\mu} &= \frac{\partial \eta}{\partial k_{\mu}}, & \varepsilon_{\mu\nu} &= \frac{\partial^2 \varepsilon}{\partial k_{\mu} \partial k_{\nu}}, & \theta_{\mu\nu} &= \frac{\partial^2 \theta}{\partial k_{\mu} \partial k_{\nu}}, \\ E_{\mu\nu} &= \frac{\partial^2 E}{\partial k_{\mu} \partial k_{\nu}}, & \Delta_{\mu\nu} &= \frac{\partial^2 \Delta}{\partial k_{\mu} \partial k_{\nu}}, & \eta_{\mu\nu} &= \frac{\partial^2 \eta}{\partial k_{\mu} \partial k_{\nu}}, \end{aligned} \quad (32)$$

for $\mu, \nu = x$ or y . For example, using the formula (F3) in Appendix B, we obtain the Berry curvature as

$$\Omega_{\pm\sigma} = \mp \frac{\varepsilon}{E} (\theta_x \eta_y - \theta_y \eta_x) + O(s^2), \quad (33)$$

On the other hand, using the formulae (F1) and (F7) in Appendix B, the diagonal matrix element of magnetic moment $M_{\pm \pm \sigma}$ becomes

$$M_{\pm \pm \sigma} = \frac{e}{2\hbar} (\Delta_x \theta_y - \Delta_y \theta_x) + \frac{e\hbar}{2m} \sigma + O(s^2). \quad (34)$$

Here we have used a relation

$$\frac{\Delta}{E} E_{\mu} - 2\varepsilon \eta_{\mu} = \Delta_{\mu}, \quad (35)$$

which are shown in Appendix C. Other useful relations are also shown in Appendix C.

From the explicit forms of E , $\Omega_{\pm\sigma}$, and $M_{\pm \pm \sigma}$, it is straightforward to write down χ_{LP} , $\chi_{\text{FS-P}}$, and χ_{occ2} . χ_{FS} and χ_{occ1} are shown in Appendix D, where we have used the integral formulae in Appendix B. χ_{inter} contains the summation over $E_{l'\mathbf{k}\sigma}$ and $u_{l'\mathbf{k}\sigma}$, which are the other energy dispersions and wave functions than for the two

bands forming the Dirac dispersion. We can calculate the summation over l' without using the explicit expression

of $u_{l'\mathbf{k}\sigma}$ by making use of the completeness condition,

$$u_{\mathbf{k}\sigma}^+(\mathbf{r})u_{\mathbf{k}\sigma}^{+*}(\mathbf{r}') + u_{\mathbf{k}\sigma}^-(\mathbf{r})u_{\mathbf{k}\sigma}^{-*}(\mathbf{r}') + \sum_{l' \neq \pm, \sigma} u_{l'\mathbf{k}\sigma}(\mathbf{r})u_{l'\mathbf{k}\sigma}^*(\mathbf{r}') = \delta(\mathbf{r} - \mathbf{r}'). \quad (36)$$

The details of calculations are shown in Appendix E.

χ_{total} [Eq. (1)] is calculated in Appendix D, which is classified into a few groups as follows:

$$\chi_{\text{total}} = \chi_{\text{LP}} + \chi_{\text{Pauli}} + \chi_{\text{OZ}} + \chi_{\text{atomic}} + \chi_1 + \chi_2, \quad (37)$$

with

$$\chi_{\text{LP}} = \frac{e^2}{12\hbar^2} \sum_{\pm, \mathbf{k}\sigma} f'(\pm E) [E_{xx}E_{yy} - E_{xy}^2], \quad (38)$$

$$\chi_{\text{Pauli}} = -\frac{e^2\hbar^2}{4m^2} \sum_{\pm, \mathbf{k}\sigma} f'(\pm E), \quad (39)$$

$$\chi_{\text{OZ}} = \frac{e^2}{m} \sum_{\pm, \mathbf{k}, \sigma} f'(\pm E) \sigma \varepsilon (\eta_x \theta_y - \eta_y \theta_x) - \frac{e^2}{m} \sum_{\pm, \mathbf{k}, \sigma} f(\pm E) \sigma \Omega_{\pm\sigma} + O(s^2), \quad (40)$$

$$\chi_{\text{atomic}} = -\frac{e^2}{4m} \sum_{\pm, \mathbf{k}, \sigma} f(\pm E) \langle x^2 + y^2 \rangle = -\frac{3e^2 a_{\text{B}}^{*2}}{m} n(\mu) + O(s^2) \quad (41)$$

$$\begin{aligned} \chi_1 = & \frac{e^2}{\hbar^2} \sum_{\pm, \mathbf{k}, \sigma} f(\pm E) \left[\pm \frac{\eta_x^2}{2E} (\varepsilon \varepsilon_{yy} + \Delta \Delta_{yy}) \mp \frac{\eta_x \eta_y}{2E} (\varepsilon \varepsilon_{xy} + \Delta \Delta_{xy}) \mp \frac{\varepsilon \Delta}{4E} (\eta_x \theta_x \theta_{yy} - \eta_x \theta_y \theta_{xy}) \right. \\ & \left. \pm \frac{1}{8} (E_x \theta_x \theta_{yy} - E_x \theta_y \theta_{xy}) \mp \frac{\theta_x^2}{8E} (\Delta \Delta_{yy} + 2\varepsilon \Delta_y \eta_y) \pm \frac{\theta_x \theta_y}{8E} (\Delta \Delta_{xy} + 2\varepsilon \Delta_x \eta_y) \right] + (x \leftrightarrow y) \\ & + \frac{e^2}{\hbar^2} \sum_{\pm \mathbf{k}\sigma} f'(\pm E) \left[\frac{\varepsilon^2 E_x}{8E} (\theta_y \theta_{xy} - \theta_x \theta_{yy}) + \frac{\Delta E_x}{8E} (\Delta_x \theta_y^2 - \Delta_y \theta_x \theta_y) \right. \\ & \left. + \frac{E_x}{4E} \{ \eta_y (\Delta \varepsilon_{xy} - \varepsilon \Delta_{xy}) - \eta_x (\Delta \varepsilon_{yy} - \varepsilon \Delta_{yy}) \} - \frac{1}{4} (\theta_x^2 \Delta_y^2 - \theta_x \theta_y \Delta_x \Delta_y) \right] + (x \leftrightarrow y) + O(s^2), \quad (42) \end{aligned}$$

$$\chi_2 = \frac{e^2}{\hbar^2} \sum_{\pm, \mathbf{k}, \sigma} f(\pm E) \left[\mp \frac{\langle y^2 \rangle}{4E} (-a^2 \varepsilon^2 + \Delta \Delta_{xx} + \Delta \Delta_{yy}) \mp \frac{\hbar^2}{4m} \left(\frac{a^2 s \varepsilon^2}{2Et} - \frac{\varepsilon^2}{Et} \langle x^2 + y^2 \rangle_R \right) \right] + O(s^2). \quad (43)$$

The ‘‘expectation values’’ $\langle \dots \rangle$ and $\langle \dots \rangle_R$ are defined by

$$\langle x^2 + y^2 \rangle = \int \Phi^*(\mathbf{r})(x^2 + y^2)\Phi(\mathbf{r})d\mathbf{r}, \quad (44)$$

and

$$\langle x^2 + y^2 \rangle_R = \int \Phi^*(\mathbf{r} - \mathbf{R})(x^2 + y^2)\Phi(\mathbf{r})d\mathbf{r}, \quad (45)$$

with \mathbf{R} being one of the vectors that point adjacent sites. Note that the value $\langle x^2 + y^2 \rangle_R$ depends on $R = |\mathbf{R}|$, and does not depend on the direction of \mathbf{R} . The present result is consistent with the previous one for graphene,[24] but there appear several new contributions due to the

presence of the staggered on-site potential Δ_0 and SOI t_2 .

χ_{Pauli} is the Pauli paramagnetism and χ_{OZ} is the OZ cross term obtained in [21]. χ_{atomic} represents the contributions from the occupied states in the partially filled $2p_z$ -band, which we call ‘‘intraband atomic diamagnetism’’. [22–24] $n(\mu)$ in χ_{atomic} represents the total electron number with spin considered when the chemical potential is μ . The other contributions χ_{LP} , χ_1 and χ_2 are the primary orbital contributions. Note that in the absence of the SOI, $\Delta_x = \Delta_y = \Delta_{xx} = \Delta_{yy} = \Delta_{xy} = 0$, so that χ_1 and χ_2 become simple.

IV. NUMERICAL RESULTS

A. Chemical potential dependence

Performing the numerical integration for the \mathbf{k} -summation, we obtain the magnetic susceptibility. The parameters used are taken from the values in graphene, which are tabulated in Table I [24]. Figure 3 shows each contribution to magnetic susceptibility for some choices of parameters, $\{\Delta_0, t_2\}$: (a) $\{\Delta_0/t, t_2/t\} = \{1/2, 0\}$, (b) $\{1/4, \sqrt{3}/72\}$, and (c) $\{1/4, \sqrt{3}/24\}$ as functions of chemical potential. In each figure, the classified contributions are shown. The top figures show χ_{LP} (red, solid line), χ_1 (blue, dashed line), and χ_2 (green, dot-dashed line). The middle figures show χ_{OZ} (red, solid line), χ_{atomic} (blue, dashed line), and χ_{Pauli} (green, dot-dashed line). The bottom figures show the total contribution χ_{total} . The values are shown in units of $\chi_0 = e^2 L^2 a^2 t / (2\pi\hbar)^2$. There are several remarks on the above results.

(i) For $t_2 = 0$ case [Fig. 3 (a)], $\chi_{\text{LP}} + \chi_1$ coincides with the result by Raoux *et al.* [35], which is based on the Peierls-phase formulation. The present result has additional contributions, χ_{Pauli} , χ_2 and χ_{atomic} . Figure 4 shows $\chi_{\text{LP}} + \chi_1$ (i.e., the result by Raoux *et al.*; red, solid line), χ_{Pauli} (blue, dashed line), and $\chi_2 + \chi_{\text{atomic}}$ (green, dot-dashed line). $\chi_2 + \chi_{\text{atomic}}$ originates from the deformation of the wave functions [22–24, 26], which is not considered in the Peierls-phase formulation. This effect also exists for finite t_2 cases. Note that χ_{OZ} vanishes in this case.

(ii) The term χ_{atomic} in Eq. (41) is in the zeroth order with respect to the overlap integrals as in the square lattice and graphene cases [23, 24]. This term is proportional to the electron number of $2p_z$ band, $n(\mu)$. Since this originates from the motion of an electron in an atom, this term does not depend on the magnitude of the overlap integral or the amplitude of transfer integral. This term produces asymmetric dependence on μ .

(iii) At the band bottom ($\mu \simeq -\sqrt{9t^2 + \Delta_0^2}$), only χ_{LP} and χ_{Pauli} have contributions. The former represents the Landau-Peierls diamagnetism [27, 28], which is understood as the extension of Landau's diamagnetism for a periodic system; The latter represents Pauli paramagnetism, the magnitude of which is proportional to the density of states. The ratio of these contribution is given by $|\chi_{\text{LP}}/\chi_{\text{Pauli}}| = \frac{1}{3}(m/m^*)^2$ where m^* is the effective mass at the band bottom [45]. For $\Delta_0 = 0$ case, $m^* = 2\hbar^2/3ta$ [24] and the ratio becomes $|\chi_{\text{LP}}/\chi_{\text{Pauli}}| = 0.659$ with the parameters shown in Table I. Thus the total magnetic susceptibility is paramagnetic at the band bottom.

(iv) At the van Hove singularity ($\mu \simeq \pm t$), we observe sharp peaks in χ_{LP} , χ_{Pauli} , and χ_{OZ} . This fact suggests that χ_{OZ} is not just a small correction to the magnetic susceptibility, but one of the primary contributions. The term χ_{OZ} exists when $t_2 \neq 0$ and reflects the sign of t_2 , and its peak at the van Hove singularity can be negative for $t_2 < 0$.

(v) In χ_{total} near $\mu = 0$ shown in Fig. 3 (a)–(c), we find one plateau for $t_2 = 0$ and two plateaus for finite t_2 . These behaviors are explained as follows. First, the effective Hamiltonian in the vicinities of K and K' points is given by

$$H_{\text{eff}} = \hbar v k_x \tau_x + \hbar v k_y \tau_y + m_0 \tau_z, \quad (46)$$

where $v = 3ta/2\hbar$ is velocity and $m_0 = |\Delta_0 + 3\sqrt{3}\sigma t_2| (|\Delta_0 - 3\sqrt{3}\sigma t_2|)$ for K (K') point. For this system, the orbital magnetic susceptibility with chemical potential μ is obtained as [35]

$$\begin{aligned} \chi_{2\text{DDirac}}(\mu, T, m_0) &= \frac{3\pi t}{2|m_0|} (f(|m_0|) - f(-|m_0|)) \chi_0, \end{aligned} \quad (47)$$

$$= -\frac{3\pi t}{2|m_0|} \chi_0 \theta(|m_0| - |\mu|) \quad (T = 0). \quad (48)$$

This equation shows that $\chi_{2\text{DDirac}}(\mu, T = 0, \Delta_0)$ has a finite negative value only when μ is in the gap. For finite t_2 cases, gaps of different sizes open at K and K' points, and thus, the multi-plateau structure is formed.

(vi) For the case of $t_2 = \sqrt{3}/24$ (Fig 3(c)), apart from the contribution discussed in (v), we observe an extra diamagnetic contribution χ_{OZ} at $\mu = 0$. This condition corresponds to the topologically nontrivial state, and χ_{OZ} reflects the topological invariant of the model, the spin Chern number [46]. Note that the sign of χ_{OZ} depends on t_2 , and χ_{OZ} is not always diamagnetic. In Sec. IV C, we discuss the relation in detail.

TABLE I. Parameters for graphene that are used in the numerical integration. [24]

Parameters	Value
a	1.42
s	0.237
t	3.55
Z_{eff}	3.25

B. Scaling of the diamagnetic peak at $\mu = 0$

In this subsection, we discuss the jumps in the orbital magnetic susceptibility, i.e., $\chi_{\text{LP}} + \chi_1$, at the both ends of the gap [see Fig. 4]. (Note that χ_2 does not contribute to jump.) We denote the magnitude of the jump as $\Delta\chi_{\text{dia}}$. We expect that $\Delta\chi_{\text{dia}}$ should be equal to the jump $3\pi t \chi_0 / |m_0|$ obtained analytically in the effective Hamiltonian with two valleys considered [see Eq. (48)]. The open circles in Fig. 5 show $\Delta\chi_{\text{dia}}$ obtained from our numerical result for several values of t/Δ_0 at $t_2/t = 0.1$ and $k_B T/t = 0.001$. We can see that the open circles are excellently on the line $-3\pi t \chi_0 / \Delta_0$. (Note that $|m_0| = \Delta_0$ at $t_2 = 0$.)

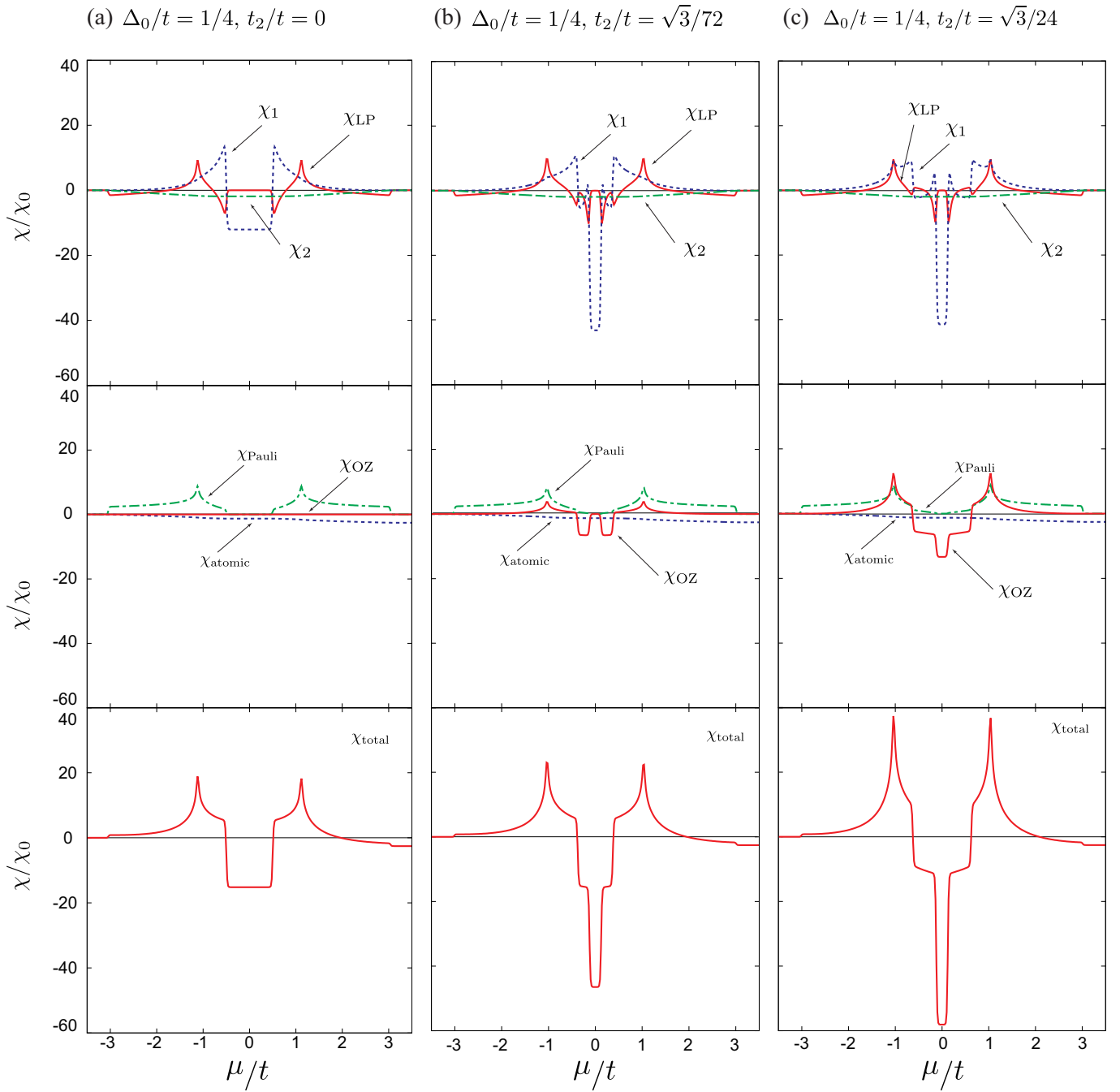


FIG. 3. Each contributions to the magnetic susceptibility as a function of the chemical potential. Top: χ_{LP} (red, solid line), χ_1 (blue, dashed line), and χ_2 (green, dot-dashed line). Middle: χ_{OZ} (red, solid line), χ_{atomic} (blue, dashed line), and χ_{Pauli} (green, dot-dashed line). Bottom: figures show the total contribution χ_{total} .

For finite t_2 cases, there are two different gaps at K and K' points, the sizes of which we denote as Δ^K and $\Delta^{K'}$, respectively. Similarly, we find the jumps in the orbital magnetic susceptibility $\chi_{LP} + \chi_1$ at the both ends of each gap, and each jump coincides with the calculated value for the corresponding gap, $\chi_{2DDirac}(\mu = 0, T, \Delta^K)$ or $\chi_{2DDirac}(\mu = 0, T, \Delta^{K'})$.

C. Relation between χ_{OZ} and the topological phase

We discuss the Berry curvature-related contribution χ_{OZ} on the basis of the discussion previously given by the authors [21]. We concentrate on the case of $T = 0$ and $\mu = 0$, where the chemical potential is located in the

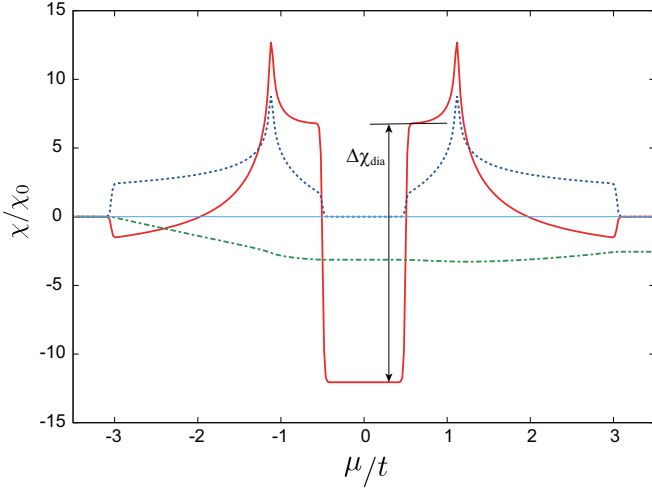


FIG. 4. Contributions to magnetic susceptibility as a function of the chemical potential at $\Delta_0 = 0.5t$ and $t_2 = 0$. The solid (red), dashed (blue), and dot-dashed (green) lines correspond to $\chi_1 + \chi_{LP}$ (i.e., the result by Raoux *et al.*), χ_{Pauli} , and χ_2 , respectively. The jump at the both ends of gap in $\chi_1 + \chi_{LP}$ is denoted as $\Delta\chi_{dia}$.

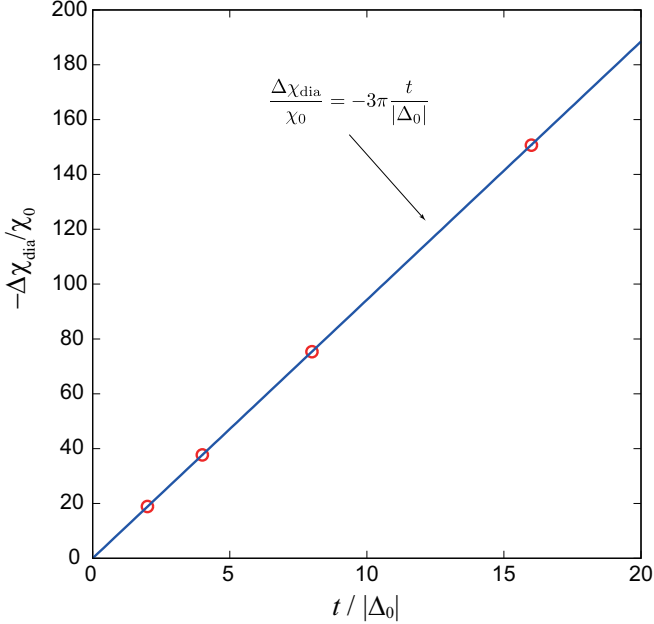


FIG. 5. Difference in magnetic susceptibility at the both ends of the gap in $\chi_1 + \chi_{LP}$, $\Delta\chi_{dia}$, as a function of t/Δ_0 at $t_2 = 0$ and $k_B T/t = 0.001$. Open circles: $\Delta\chi_{dia}$ obtained from our numerical result with $t/|\Delta_0| = 2.0, 4.0, 8.0,$ and 16.0 . Solid line: Result obtained by the continuum model Eq. (48).

gap. In this case, χ_{OZ} is given by

$$\chi_{OZ}(\mu = 0) = \frac{2e\mu_B}{\hbar} \sum_{l:\text{occupied}} \sum_{\mathbf{k}, \sigma} \sigma \Omega_{l\sigma}^z. \quad (49)$$

Note that the topology of wave functions in a spin-conserved system is characterized by the Chern number,

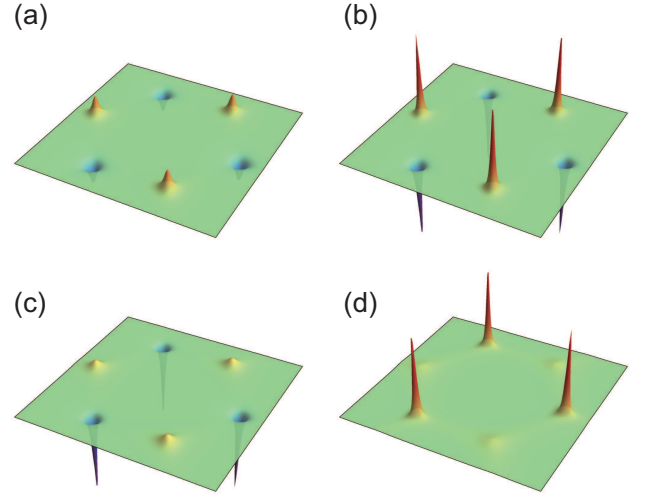


FIG. 6. The distribution of Berry curvature for the lower band with spin up at each parameter: (a) $\Delta_0/t = 1/4, t_2/t = 0$, (b) $\Delta_0/t = 1/8, t_2/t = 0$, (c) $\Delta_0/t = 1/4, t_2/t = \sqrt{3}/72$, and (d) $\Delta_0/t = 1/4, t_2/t = \sqrt{3}/24$. The integral of the Berry curvature over the whole Brillouin zone is zero when (a), (b), and (c), while the counterpart of (d) is 2π . The state is topologically non-trivial only in the case of (d).

$\text{Ch}_{l,\sigma}$, where l and σ represents the band index and spin. The Chern number is explicitly given by

$$\text{Ch}_{l,\sigma} = \frac{1}{2\pi} \int d\mathbf{k} \Omega_{l\sigma} = \frac{2\pi}{L^2} \sum_{\mathbf{k}} \Omega_{l\sigma}. \quad (50)$$

and takes an integer value. Using this relation, χ_{OZ} at $\mu = 0$ is given by

$$\chi_{OZ}(\mu = 0) = -\frac{4|e|\mu_B L^2}{\hbar} \cdot \frac{1}{2} (\text{Ch}_{\text{occ},\uparrow} - \text{Ch}_{\text{occ},\downarrow}). \quad (51)$$

The right-hand side is proportional to the spin Chern number for the occupied band, a topological invariant for 2D TIs, defined by $(\text{Ch}_{\text{occ},\uparrow} - \text{Ch}_{\text{occ},\downarrow})/2$. This result indicates that $\chi_{OZ}(\mu = 0)$ is quantized in units of the universal value, $\chi_u = 4|e|\mu_B/\hbar = 13.37\chi_0$ per area, reflecting the topological phase of materials.

Figure 6 shows the distribution of $\Omega_{l\sigma}(\mathbf{k})$ for some choices of parameters. For the case $t_2 = 0$ with different sizes of gaps [Fig. 6(a,b)], the relation of the Berry curvature $\Omega_{l\sigma}(-\mathbf{k}) = -\Omega_{l\sigma}(\mathbf{k})$ holds and the summation of $\Omega_{l\sigma}$ in the Brillouin zone vanishes. For nonzero t_2 , the relation $\Omega_{l\sigma}(-\mathbf{k}) = -\Omega_{l\sigma}(\mathbf{k})$ does not hold in general. Nevertheless, as long as $|\Delta_0| > 3\sqrt{3}|t_2|$ holds, the summation of the Berry curvature in the Brillouin zone is zero and $\chi_{OZ}(\mu = 0)$ also vanishes [Fig. 6(c)]. This corresponds to the fact that the system is still topologically trivial. On the other hand, for $|\Delta_0| < 3\sqrt{3}|t_2|$, the summation becomes nonzero [Fig. 6(d)]. In this parameter region, the system is topologically nontrivial and χ_{OZ} has a finite contribution. These results show that $\chi_{OZ}(\mu = 0)$ reflects the topological order of the Kane-Mele model.

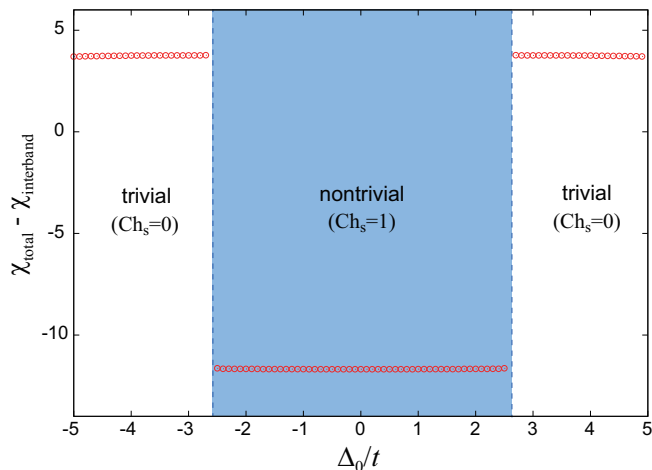


FIG. 7. Magnetic susceptibility with the interband contribution subtracted, where we define $\chi_{\text{interband}} = \chi_{2\text{DDirac}}(\mu = 0, T, \Delta^K) + \chi_{2\text{DDirac}}(\mu = 0, T, \Delta^{K'})$. The parameters t_2 and T are set to $t_2 = 0.1t$ and $k_B T = 0.001t$. The magnitude of jump mainly comes from the universal quantized value $\chi_u = 13.37\chi_0$; however, there exist an additional discontinuous contribution originating from a *purely* orbital term contained in $\chi_{\text{occ}2}$ in Eqs. (29) and (30). The overall positive shift originates from the plateau shown in Fig. 3.

As the ratio of t_2 to Δ_0 changes, a jump in $\chi_{\text{OZ}}(\mu = 0)$ occurs at the topological phase transition.

Let us discuss experimental detection of the jump. For $\mu = 0$, the primary contribution is χ_1 as well as χ_{OZ} . As shown in Sec. IV B, χ_1 diverges at the critical point $|\Delta_0| = 3\sqrt{3}|t_2|$. Although it seems difficult to detect the jump due to this divergence, χ_{OZ} will be experimentally observed according to the discussion below.

It is naturally assumed that the diverging interband contribution comes from the vicinities of K and K' points. As we mentioned, we can evaluate the contribution from K and K' at $\mu = 0$ as $\chi_{2\text{DDirac}}(\mu = 0, T, \Delta^K) + \chi_{2\text{DDirac}}(\mu = 0, T, \Delta^{K'})$. If we subtract this value from the observed total magnetic susceptibility, we obtain the residue containing the jump in χ_{OZ} , i.e., the topological phase transition-related jump. Figure 7 shows the residue obtained by the above subtraction as a function of Δ_0/t . In this way, we can find the evidence of a topological phase transition. Note that the staggered on-site potential is variable by an electric field applied perpendicularly to the 2D plane. Therefore, the magnitude of the electric field corresponds to the horizontal axis in Fig. 7.

Figure 7 indicates that the magnitude of the jump in the total contribution slightly deviates from the predicted value $13.37\chi_0$. This deviation originates from

the Berry-curvature-related term in the *purely* orbital, Berry-curvature-related contribution contained in $\chi_{\text{occ}2}$ [see Eqs. (29) and (30)], which also changes discontinuously at topological phase transitions. This fact does not contradict the statement that χ_{OZ} is universally quantized.

Note that the effect of the Berry curvature on the orbital magnetism was studied in some literatures [47–53]. In our formulation, the effect of the Berry curvature is included in χ_1 , and causes the deviation of the jump from quantized value. However, this effect is purely orbital and does not affect χ_{OZ} .

V. SUMMARY

We calculated the orbital, spin-Zeeman, and OZ magnetic susceptibility for the Kane-Mele model, using the formula written in terms of explicit wave functions, which enables us to evaluate each contribution taking account of the integration over the whole Brillouin zone and the summation over all the bands. The result includes additional contributions to the previous results [21], such as core electron diamagnetism, originating from the deformation of the wave functions by an external field. Furthermore, the numerical calculation has revealed the following:

- (1) The quantization of the OZ cross term is confirmed. If we can evaluate the size of the gap with some methods, we will be able to detect the OZ cross term experimentally and observe the change in the spin Chern number directly.
- (2) The OZ cross term can be a relatively large contribution, especially for insulating states and at the van Hove singularity, and is one of the primary contributions to the magnetic susceptibility.

The present study clarifies the behavior of the OZ cross term and its magnitude compared with the other contributions. We expect that the OZ cross term will serve as a useful tool for experimental studies on TIs.

ACKNOWLEDGMENTS

We thank very fruitful discussions with H. Matsuura, H. Maebashi, I. Tateishi, T. Hirotsawa, N. Okuma, and V. Könye. This work was supported by Grants-in-Aid for Scientific Research from the Japan Society for the Promotion of Science (Grants No. JP18H01162). S.O. was supported by the Japan Society for the Promotion of Science through the Program for Leading Graduate Schools (MERIT).

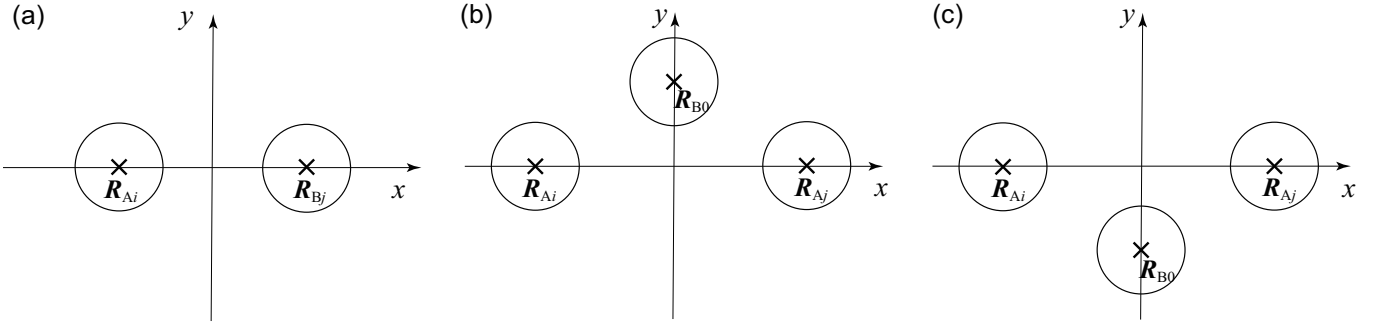


FIG. 8. Configurations of atoms for (a) nearest-neighbor and (b), (c) next-nearest-neighbor hoppings.

Appendix A: Hopping integrals due to the spin-orbit interaction

In this Appendix, we obtain hopping integrals due to the spin orbit interaction using LCAO in Eqs. (8) and (9). The matrix elements of SOI in Eq. (3) between $\varphi_{A\mathbf{k}}(\mathbf{r})$ and $\varphi_{B\mathbf{k}}(\mathbf{r})$ is given by

$$h_{AB\sigma\sigma'}^{\text{SO}}(\mathbf{k}) \simeq \frac{1}{N} \sum_{\mathbf{R}_{Ai}, \mathbf{R}_{Bj}} e^{-i\mathbf{k}(\mathbf{R}_{Ai} - \mathbf{R}_{Bj})} \int d\mathbf{r} \Phi_{\sigma}^*(\mathbf{r} - \mathbf{R}_{Ai}) \frac{\hbar^2}{4m^2c^2} \times (\boldsymbol{\sigma})_{\sigma\sigma'} \cdot \nabla \{V_A(\mathbf{r} - \mathbf{R}_{Ai}) + V_B(\mathbf{r} - \mathbf{R}_{Bj})\} \times \{-i\nabla\Phi_{\sigma'}(\mathbf{r} - \mathbf{R}_{Bj})\}, \quad (\text{A1})$$

where we have chosen $V_A(\mathbf{r} - \mathbf{R}_{Ai}) + V_B(\mathbf{r} - \mathbf{R}_{Bj})$ out of $V(\mathbf{r})$ since the other terms in $V(\mathbf{r})$ should be small at $\mathbf{r} = \mathbf{R}_{Ai}$ or $\mathbf{r} = \mathbf{R}_{Bj}$. We show the spin component of the wave functions explicitly. Other matrix elements $h_{AA\sigma\sigma'}^{\text{SO}}(\mathbf{k})$ and $h_{BB\sigma\sigma'}^{\text{SO}}(\mathbf{k})$ are expressed in similar ways, which are to be discussed later.

The dominant contribution in Eq. (A1) is between the nearest-neighbor-sites. By choosing an appropriate coordinates, the \mathbf{r} integral can be expressed as in Fig. 8(a). We can assume that $V_A(\mathbf{r} - \mathbf{R}_{Ai})$, $V_B(\mathbf{r} - \mathbf{R}_{Bj})$, $\Phi_{\sigma}(\mathbf{r} - \mathbf{R}_{Ai})$ and $\Phi_{\sigma'}(\mathbf{r} - \mathbf{R}_{Bj})$ are even functions with respect to y . Therefore, when one of the two nablas in Eq. (A1) is $\frac{\partial}{\partial y}$, the \mathbf{r} integral vanishes. We can also assume that $V_A(\mathbf{r} - \mathbf{R}_{Ai})$ and $V_B(\mathbf{r} - \mathbf{R}_{Bj})$ are even functions with respect to z , while $\Phi_{\sigma}(\mathbf{r} - \mathbf{R}_{Ai})$ and $\Phi_{\sigma'}(\mathbf{r} - \mathbf{R}_{Bj})$ are odd functions. Therefore, when one of the two nablas in Eq. (A1) is $\frac{\partial}{\partial z}$, the \mathbf{r} integral vanishes again. As a result, $h_{AB\sigma\sigma'}^{\text{SO}}(\mathbf{k})$ vanishes.

Next, we discuss $h_{AA\sigma\sigma'}^{\text{SO}}(\mathbf{k})$. The dominant contribution is between the next-nearest-neighbor pair,

$$h_{AA\sigma\sigma'}^{\text{SO}}(\mathbf{k}) \simeq \frac{1}{N} \sum_{\mathbf{R}_{Ai}, \mathbf{R}_{Aj}} e^{-i\mathbf{k}(\mathbf{R}_{Ai} - \mathbf{R}_{Aj})} \int d\mathbf{r} \Phi_{\sigma}^*(\mathbf{r} - \mathbf{R}_{Ai}) \frac{\hbar^2}{4m^2c^2} \times (\boldsymbol{\sigma})_{\sigma\sigma'} \cdot \nabla \{V_A(\mathbf{r} - \mathbf{R}_{Ai}) + V_B(\mathbf{r} - \mathbf{R}_{B0}) + V_A(\mathbf{r} - \mathbf{R}_{Aj})\} \times \{-i\nabla\Phi_{\sigma'}(\mathbf{r} - \mathbf{R}_{Aj})\}. \quad (\text{A2})$$

The appropriate coordinates give the configurations as in Fig. 8(b) and (c). In the following, we neglect the overlap integral s in $\Phi_{\sigma}(\mathbf{r})$ and replace $\Phi_{\sigma}(\mathbf{r})$ with $\phi_{\sigma}(\mathbf{r})$. All the potentials in Eq. (A2) will be even functions with respect to z , while $\phi_{\sigma}^*(\mathbf{r} - \mathbf{R}_{Ai})$ and $\phi_{\sigma'}(\mathbf{r} - \mathbf{R}_{Aj})$ are odd functions. Therefore, as in the case of Eq. (A1), when one of the two nablas is $\frac{\partial}{\partial z}$, the \mathbf{r} integral vanishes. Similarly, the terms in Eq. (A2) with $V_A(\mathbf{r} - \mathbf{R}_{Ai})$ and $V_A(\mathbf{r} - \mathbf{R}_{Aj})$ are even functions with respect to y . Therefore they vanish as in the case of Eq. (A1). In contrast, the term with $V_B(\mathbf{r} - \mathbf{R}_{B0})$ gives a nonzero value,

$$\frac{\hbar^2}{4m^2c^2} \int d\mathbf{r} \phi_{\sigma}^*(\mathbf{r} - \mathbf{R}_{Ai})(\sigma^z)_{\sigma\sigma'} \left[\frac{\partial}{\partial x} V_B(\mathbf{r} - \mathbf{R}_{B0}) \left(-i \frac{\partial}{\partial y} \right) \phi_{\sigma'}(\mathbf{r} - \mathbf{R}_{Aj}) - \frac{\partial}{\partial y} V_B(\mathbf{r} - \mathbf{R}_{B0}) \left(-i \frac{\partial}{\partial x} \right) \phi_{\sigma'}(\mathbf{r} - \mathbf{R}_{Aj}) \right] d\mathbf{r}. \quad (\text{A3})$$

If we assume $\mathbf{R}_{B0} = (0, b, 0)$, $\mathbf{R}_{Aj} = (a, 0, 0)$, $V_B(\mathbf{r} - \mathbf{R}_{B0}) = V_B(\rho, z)$, and $\phi_{\sigma'}(\mathbf{r} - \mathbf{R}_{Aj}) = \phi_{\sigma'}(\rho_A, z)$ with $\rho = \sqrt{x^2 + (y - b)^2}$ and $\rho_A = \sqrt{(x - a)^2 + y^2}$ for Fig. 8(b), the integral in Eq. (A3) becomes

$$-i \int d\mathbf{r} \phi_{\sigma}^*(\mathbf{r} - \mathbf{R}_{Ai})(\sigma^z)_{\sigma\sigma'} (ay + bx - ab) \frac{1}{\rho\rho_A} \frac{\partial V_B(\rho, z)}{\partial \rho} \frac{\partial \phi_{\sigma'}(\rho_A, z)}{\partial \rho_A}. \quad (\text{A4})$$

Similarly, for Fig. 8(c), we obtain

$$-i \int d\mathbf{r} \phi_{\sigma}^*(\mathbf{r} - \mathbf{R}_{Ai}) (\sigma^z)_{\sigma\sigma'} (ay - bx + ab) \frac{1}{\rho' \rho_A} \frac{\partial V_B(\rho', z)}{\partial \rho'} \frac{\partial \phi_{\sigma'}(\rho_A, z)}{\partial \rho_A}, \quad (\text{A5})$$

with $\rho' = \sqrt{x^2 + (y+b)^2}$. When we make the change of the integral variable $y \rightarrow -y$, we can see that Eq. (A5) exactly equals (-1) times Eq. (A4). In the same way, we can obtain $h_{\text{BB}\sigma\sigma'}^{\text{SO}}(\mathbf{k})$. These next-nearest-neighbor hoppings exactly have the same symmetry as Kane-Mele assumed, although the absolute value and the sign is determined from the details of the functional forms in Eq. (A3).

Appendix B: Integration Formulae

Table II shows the order estimates of several quantities with respect to the ‘‘overlap integrals’’ s , t or t_2 (all denoted as s in the following) for the two cases of $\Delta_0 \gg t$ and $\Delta_0 \lesssim t$. Note that $E_{\mathbf{k}\sigma} = \sqrt{\Delta_{\mathbf{k}\sigma}^2 + \varepsilon_{\mathbf{k}}^2}$. In the following calculations, we keep the terms up to the order of s^1 .

TABLE II. Order estimations of several quantities with respect to the ‘‘overlap integral’’ s , t , or t_2 (all denoted as s). Here μ is x or y , and $\eta_{\mathbf{k}\sigma}$ and $\theta_{\mathbf{k}}$ are defined in Eqs. (21)-(23).

	$\Delta_0 \gg t$	$\Delta_0 \lesssim t$
$E_{\mathbf{k}\sigma}$	1	s
$\frac{\partial E_{\mathbf{k}\sigma}}{\partial k_{\mu}}$	s	s
$\eta_{\mathbf{k}\sigma}$	1	1
$\frac{\partial \eta_{\mathbf{k}\sigma}}{\partial k_{\mu}}$	s	1
$\theta_{\mathbf{k}}$	1	1
$\frac{\partial \theta_{\mathbf{k}}}{\partial k_{\mu}}$	1	1
$\Delta_{\mathbf{k}\sigma}$	1	s
$\frac{\partial \Delta_{\mathbf{k}\sigma}}{\partial k_{\mu}}$	s	s

First, we show several integration formulae using $u_{\mathbf{k}\sigma}^{\pm}(\mathbf{r})$ of Eqs. (19) and (20), which will be used in calculating χ . To simplify the expressions, we abbreviate $\varepsilon_{\mathbf{k}}$, $\theta_{\mathbf{k}}$, $E_{\mathbf{k}\sigma}$, $\Delta_{\mathbf{k}\sigma}$, and $\eta_{\mathbf{k}\sigma}$ as ε , θ , E , Δ , and η , respectively, in the following Appendices. Furthermore, we use the abbreviations,

$$\varepsilon_{\mu} = \frac{\partial \varepsilon}{\partial k_{\mu}}, \quad \theta_{\mu} = \frac{\partial \theta}{\partial k_{\mu}}, \quad E_{\mu} = \frac{\partial E}{\partial k_{\mu}}, \quad \Delta_{\mu} = \frac{\partial \Delta}{\partial k_{\mu}}, \quad \eta_{\mu} = \frac{\partial \eta}{\partial k_{\mu}}, \quad (\text{B1})$$

$$\varepsilon_{\mu\nu} = \frac{\partial^2 \varepsilon}{\partial k_{\mu} \partial k_{\nu}}, \quad \theta_{\mu\nu} = \frac{\partial^2 \theta}{\partial k_{\mu} \partial k_{\nu}}, \quad E_{\mu\nu} = \frac{\partial^2 E}{\partial k_{\mu} \partial k_{\nu}}, \quad \Delta_{\mu\nu} = \frac{\partial^2 \Delta}{\partial k_{\mu} \partial k_{\nu}}, \quad \eta_{\mu\nu} = \frac{\partial^2 \eta}{\partial k_{\mu} \partial k_{\nu}}, \quad (\text{B2})$$

for $\mu, \nu = x$ or y . Then we obtain

$$\begin{aligned}
\text{(F1)} \quad & \int u_{\mathbf{k}\sigma}^{\pm*} \frac{\partial u_{\mathbf{k}\sigma}^{\pm}}{\partial k_{\mu}} d\mathbf{r} = \pm i \frac{\Delta}{2E} \theta_{\mu} + O(s^2), \\
\text{(F2)} \quad & \int u_{\mathbf{k}\sigma}^{\pm*} \frac{\partial u_{\mathbf{k}\sigma}^{\mp}}{\partial k_{\mu}} d\mathbf{r} = i \frac{\varepsilon}{2E} \theta_{\mu} \pm \eta_{\mu} + O(s^2), \\
\text{(F3)} \quad & \int \frac{\partial u_{\mathbf{k}\sigma}^{\pm*}}{\partial k_{\mu}} \frac{\partial u_{\mathbf{k}\sigma}^{\pm}}{\partial k_{\nu}} d\mathbf{r} = \langle x_{\mu} x_{\nu} \rangle + \frac{1}{4} \theta_{\mu} \theta_{\nu} + \eta_{\mu} \eta_{\nu} \pm i \frac{\varepsilon}{2E} (\theta_{\mu} \eta_{\nu} - \theta_{\nu} \eta_{\mu}) \mp \frac{\varepsilon}{E} \text{Re} X_{\mu\nu} + O(s^2), \\
\text{(F4)} \quad & \int \frac{\partial u_{\mathbf{k}\sigma}^{\pm*}}{\partial k_{\mu}} \frac{\partial u_{\mathbf{k}\sigma}^{\mp}}{\partial k_{\nu}} d\mathbf{r} = -i \frac{\Delta}{2E} (\theta_{\mu} \eta_{\nu} - \theta_{\nu} \eta_{\mu}) + Y_{\mu\nu}^{\pm} + O(s^2), \\
\text{(F5)} \quad & \int u_{\mathbf{k}\sigma}^{\pm*} \frac{\partial H_{\mathbf{k}}}{\partial k_{\mu}} u_{\mathbf{k}\sigma}^{\pm} d\mathbf{r} = \pm E_{\mu}, \\
\text{(F6)} \quad & \int u_{\mathbf{k}\sigma}^{\pm*} \frac{\partial H_{\mathbf{k}}}{\partial k_{\mu}} u_{\mathbf{k}\sigma}^{\mp} d\mathbf{r} = \mp 2E \int u_{\mathbf{k}\sigma}^{\pm*} \frac{\partial u_{\mathbf{k}\sigma}^{\mp}}{\partial k_{\mu}} d\mathbf{r} = \mp i \varepsilon \theta_{\mu} - 2E \eta_{\mu} + O(s^2), \\
\text{(F7)} \quad & \int u_{\mathbf{k}\sigma}^{\pm*} \frac{\partial H_{\mathbf{k}}}{\partial k_{\mu}} \frac{\partial u_{\mathbf{k}\sigma}^{\pm}}{\partial k_{\nu}} d\mathbf{r} = -\frac{\hbar^2}{2m} \delta_{\mu\nu} \pm \frac{1}{2} E_{\mu\nu} + i \frac{\Delta}{2E} E_{\mu} \theta_{\nu} - i \varepsilon (\eta_{\mu} \theta_{\nu} - \eta_{\nu} \theta_{\mu}) + O(s^2), \\
\text{(F8)} \quad & \int u_{\mathbf{k}\sigma}^{\mp*} \frac{\partial H_{\mathbf{k}}}{\partial k_{\mu}} \frac{\partial u_{\mathbf{k}\sigma}^{\pm}}{\partial k_{\nu}} d\mathbf{r} = \pm \frac{i}{2} \varepsilon_{\nu} \theta_{\mu} - \eta_{\mu} E_{\nu} - E \eta_{\mu\nu} \mp E Y_{\mu\nu}^{\mp} \pm \frac{i}{2} \varepsilon \theta_{\mu\nu} + O(s^2), \tag{B3}
\end{aligned}$$

with

$$\begin{aligned}
X_{\mu\nu} &= \sum_{\mathbf{R}} e^{-i\theta_{\mathbf{k}}} e^{-i\mathbf{k}\cdot\mathbf{R}} \langle x_{\mu} x_{\nu} \rangle_{\mathbf{R}}, \\
Y_{\mu\nu}^{\pm} &= \frac{\Delta}{E} \text{Re} X_{\mu\nu} \pm i \text{Im} X_{\mu\nu}. \tag{B4}
\end{aligned}$$

The meaning of the \mathbf{R} summation and $\langle \dots \rangle_{\mathbf{R}}$ are shown below. $X_{\mu\nu}$ and $Y_{\mu\nu}^{\pm}$ are in the order of s .

1. Derivation of (F1)-(F4)

The k_{μ} derivative of $u_{\mathbf{k}\sigma}^{+}$ becomes

$$\frac{\partial u_{\mathbf{k}\sigma}^{+}}{\partial k_{\mu}} = \frac{i}{2} \theta_{\mu} \cos 2\eta u_{\mathbf{k}\sigma}^{+} + \left(\frac{i}{2} \theta_{\mu} \sin 2\eta - \eta_{\mu} \right) u_{\mathbf{k}\sigma}^{-} + e^{\frac{i}{2}\theta} \cos \eta \frac{\partial \varphi_{\mathbf{A}\mathbf{k}}}{\partial k_{\mu}} - e^{-\frac{i}{2}\theta} \sin \eta \frac{\partial \varphi_{\mathbf{B}\mathbf{k}}}{\partial k_{\mu}}. \tag{B5}$$

To obtain (F1), we must calculate the integral of product of Bloch wavefunction $u_{\mathbf{k}\sigma}^{\pm}$ and k -derivative of $\varphi_{\mathbf{A}/\mathbf{B}\mathbf{k}}(\mathbf{r})$. They become

$$\begin{aligned}
\int u_{\mathbf{k}\sigma}^{+*} \frac{\partial \varphi_{\mathbf{A}\mathbf{k}}}{\partial k_{\mu}} d\mathbf{r} &= -e^{-\frac{i}{2}\theta} \cos \eta \frac{i}{N} \sum_{\mathbf{R}_{\mathbf{A}i}, \mathbf{R}_{\mathbf{A}j}} e^{-i\mathbf{k}(\mathbf{R}_{\mathbf{A}i} - \mathbf{R}_{\mathbf{A}j})} \int (x - R_{\mathbf{A}jx}) \Phi^{*}(\mathbf{r} - \mathbf{R}_{\mathbf{A}i}) \Phi(\mathbf{r} - \mathbf{R}_{\mathbf{A}j}) d\mathbf{r} \\
&+ e^{\frac{i}{2}\theta} \sin \eta \frac{i}{N} \sum_{\mathbf{R}_{\mathbf{A}j}, \mathbf{R}_{\mathbf{B}i}} e^{i\mathbf{k}(\mathbf{R}_{\mathbf{A}j} - \mathbf{R}_{\mathbf{B}i})} \int (x - R_{\mathbf{A}jx}) \Phi^{*}(\mathbf{r} - \mathbf{R}_{\mathbf{B}i}) \Phi(\mathbf{r} - \mathbf{R}_{\mathbf{A}j}) d\mathbf{r}. \tag{B6}
\end{aligned}$$

Hereafter, we only consider the on-site and adjacent-site contributions. Then we obtain

$$\begin{aligned}
\int u_{\mathbf{k}\sigma}^{+*} \frac{\partial \varphi_{\mathbf{A}\mathbf{k}}}{\partial k_{\mu}} d\mathbf{r} &= -e^{-\frac{i}{2}\theta} \cos \eta \frac{i}{N} \sum_{\mathbf{R}_{\mathbf{A}i}} \int (x - R_{\mathbf{A}ix}) \Phi^{*}(\mathbf{r} - \mathbf{R}_{\mathbf{A}i}) \Phi(\mathbf{r} - \mathbf{R}_{\mathbf{A}i}) d\mathbf{r} \\
&+ e^{\frac{i}{2}\theta} \sin \eta \frac{i}{N} \sum_{\substack{\mathbf{R}_{\mathbf{A}j}, \mathbf{R}_{\mathbf{B}i} \\ \mathbf{R}_{\mathbf{A}j} - \mathbf{R}_{\mathbf{B}i} = n.n.}} e^{i\mathbf{k}(\mathbf{R}_{\mathbf{A}j} - \mathbf{R}_{\mathbf{B}i})} \int (x - R_{\mathbf{A}jx}) \Phi^{*}(\mathbf{r} - \mathbf{R}_{\mathbf{B}i}) \Phi(\mathbf{r} - \mathbf{R}_{\mathbf{A}j}) d\mathbf{r} \\
&= -ie^{-\frac{i}{2}\theta} \cos \eta \langle x \rangle + i \sin \eta \sum_{\mathbf{R}} e^{i\mathbf{k}\mathbf{R}} \langle x \rangle_{(-\mathbf{R})}, \tag{B7}
\end{aligned}$$

where \mathbf{R} runs over the three vectors from a B site to its adjacent A sites. The expectation values $\langle O \rangle$ and $\langle O \rangle_{\mathbf{R}}$ are defined as [23, 24]

$$\langle O \rangle = \int \Phi^*(\mathbf{r}) \hat{O} \Phi(\mathbf{r}) d\mathbf{r}, \quad (\text{B8})$$

and

$$\langle O \rangle_{\mathbf{R}} = \int d\mathbf{r} \Phi^*(\mathbf{r} - \mathbf{R}) \hat{O} \Phi(\mathbf{r}) d\mathbf{r}. \quad (\text{B9})$$

We can see that $\langle x \rangle$ and $\langle x \rangle_{\mathbf{R}}$ are in the order of s^2 . Therefore, we obtain

$$\int u_{\mathbf{k}\sigma}^{+*} \frac{\partial \varphi_{\mathbf{A}\mathbf{k}}}{\partial k_{\mu}} d\mathbf{r} = O(s^2). \quad (\text{B10})$$

For $\partial \varphi_{\mathbf{B}\mathbf{k}} / \partial k_{\mu}$, we have the similar relation

$$\int u_{\mathbf{k}\sigma}^{+*} \frac{\partial \varphi_{\mathbf{B}\mathbf{k}}}{\partial k_{\mu}} d\mathbf{r} = O(s^2). \quad (\text{B11})$$

Using Eqs. (B10) and (B11), we have

$$\int u_{\mathbf{k}\sigma}^{+*} \frac{\partial u_{\mathbf{k}\sigma}^+}{\partial k_{\mu}} d\mathbf{r} = \frac{i}{2} \theta_{\mu} \cos 2\eta + O(s^2), \quad (\text{B12})$$

and

$$\int u_{\mathbf{k}\sigma}^{+*} \frac{\partial u_{\mathbf{k}\sigma}^-}{\partial k_{\mu}} d\mathbf{r} = \frac{i}{2} \theta_{\mu} \sin 2\eta + \eta_{\mu} + O(s^2). \quad (\text{B13})$$

If we substitute $\eta \rightarrow \eta - \pi/2$, $u_{\mathbf{k}\sigma}^+$ and $u_{\mathbf{k}\sigma}^-$ become $u_{\mathbf{k}\sigma}^-$ and $-u_{\mathbf{k}\sigma}^+$, respectively. With the relations

$$\sin 2\eta = \frac{\varepsilon}{E}, \quad \cos 2\eta = \frac{\Delta}{E}, \quad (\text{B14})$$

we obtain (F1) and (F2).

Similarly to the derivation of (F1) and (F2), we obtain

$$\int \frac{\partial \varphi_{\mathbf{A}\mathbf{k}}^*}{\partial k_{\mu}} \frac{\partial \varphi_{\mathbf{A}\mathbf{k}}}{\partial k_{\nu}} d\mathbf{r} = \int \frac{\partial \varphi_{\mathbf{B}\mathbf{k}}^*}{\partial k_{\mu}} \frac{\partial \varphi_{\mathbf{B}\mathbf{k}}}{\partial k_{\nu}} d\mathbf{r} = \langle x_{\mu} x_{\nu} \rangle + O(s^2), \quad (\text{B15})$$

and

$$\int \frac{\partial \varphi_{\mathbf{A}\mathbf{k}}^*}{\partial k_{\mu}} \frac{\partial \varphi_{\mathbf{B}\mathbf{k}}}{\partial k_{\nu}} d\mathbf{r} = \sum_{\mathbf{R}} e^{-i\mathbf{k} \cdot \mathbf{R}} \langle x_{\mu} x_{\nu} \rangle_{\mathbf{R}} + O(s^2). \quad (\text{B16})$$

Using these relations and substitution of $\eta \rightarrow \eta - \pi/2$, we obtain (F3) and (F4). In the different sign cases (e.g., $\int \frac{\partial u_{\mathbf{k}\sigma}^{+*}}{\partial k_{\mu}} \frac{\partial u_{\mathbf{k}\sigma}^-}{\partial k_{\nu}} d\mathbf{r}$), we can calculate the integral in almost the same way.

2. Derivation of (F5) and (F6)

We start from the Schrödinger equation,

$$H_{\mathbf{k}} u_{\mathbf{k}\sigma}^{\pm} = \pm E u_{\mathbf{k}\sigma}^{\pm}. \quad (\text{B17})$$

Differentiating the both sides of this equation by k_{μ} , we obtain

$$\left(\frac{\partial H_{\mathbf{k}}}{\partial k_{\mu}} \mp \frac{\partial E}{\partial k_{\mu}} \right) u_{\mathbf{k}\sigma}^{\pm} = (\pm E - H_{\mathbf{k}}) \frac{\partial u_{\mathbf{k}\sigma}^{\pm}}{\partial k_{\mu}}. \quad (\text{B18})$$

When we multiply $u_{\mathbf{k}\sigma}^{\pm*}$ and integrate the product, we obtain (F5). Similarly, multiplying $u_{\mathbf{k}\sigma}^{\mp*}$ and using (F2), we obtain (F6).

3. Derivation of (F7)

To obtain (F7), we first calculate

$$\int u_{\mathbf{k}\sigma}^{\pm*} \left(\frac{\partial H_{\mathbf{k}}}{\partial k_{\mu}} \frac{\partial u_{\mathbf{k}\sigma}^{\pm}}{\partial k_{\nu}} + \frac{\partial H_{\mathbf{k}}}{\partial k_{\nu}} \frac{\partial u_{\mathbf{k}\sigma}^{\pm}}{\partial k_{\mu}} \right) d\mathbf{r} \quad (\text{B19})$$

and

$$\int u_{\mathbf{k}\sigma}^{\pm*} \left(\frac{\partial H_{\mathbf{k}}}{\partial k_{\mu}} \frac{\partial u_{\mathbf{k}\sigma}^{\pm}}{\partial k_{\nu}} - \frac{\partial H_{\mathbf{k}}}{\partial k_{\nu}} \frac{\partial u_{\mathbf{k}\sigma}^{\pm}}{\partial k_{\mu}} \right) d\mathbf{r}. \quad (\text{B20})$$

Differentiating the both sides of Eq. (B18) by k_{ν} , we obtain

$$\left(\frac{\hbar^2}{m} \delta_{\mu\nu} \mp \frac{\partial^2 E}{\partial k_{\mu} \partial k_{\nu}} \right) u_{\mathbf{k}\sigma}^{\pm} + \left(\frac{\partial H_{\mathbf{k}}}{\partial k_{\mu}} \mp \frac{\partial E}{\partial k_{\mu}} \right) \frac{\partial u_{\mathbf{k}\sigma}^{\pm}}{\partial k_{\nu}} + \left(\frac{\partial H_{\mathbf{k}}}{\partial k_{\nu}} \mp \frac{\partial E}{\partial k_{\nu}} \right) \frac{\partial u_{\mathbf{k}\sigma}^{\pm}}{\partial k_{\mu}} + (H_{\mathbf{k}} \mp E) \frac{\partial^2 u_{\mathbf{k}\sigma}^{\pm}}{\partial k_{\mu} \partial k_{\nu}} = 0. \quad (\text{B21})$$

Here we have used the relation

$$\frac{\partial^2 H_{\mathbf{k}}}{\partial k_{\mu} \partial k_{\nu}} = \frac{\hbar^2}{m} \delta_{\mu\nu}. \quad (\text{B22})$$

Then, multiplying $u_{\mathbf{k}\sigma}^{\pm*}$ and integrating, we obtain

$$\int u_{\mathbf{k}\sigma}^{\pm*} \left(\frac{\partial H_{\mathbf{k}}}{\partial k_{\mu}} \frac{\partial u_{\mathbf{k}\sigma}^{\pm}}{\partial k_{\nu}} + \frac{\partial H_{\mathbf{k}}}{\partial k_{\nu}} \frac{\partial u_{\mathbf{k}\sigma}^{\pm}}{\partial k_{\mu}} \right) d\mathbf{r} = -\frac{\hbar^2}{m} \delta_{\mu\nu} \pm E_{\mu\nu} + i \frac{\Delta}{2E} (E_{\mu} \theta_{\nu} + E_{\nu} \theta_{\mu}) + O(s^2). \quad (\text{B23})$$

Here we have used the formula (F1).

Next, we calculate Eq. (B20). By using the explicit forms of $\frac{\partial H_{\mathbf{k}}}{\partial k_y}$ and $\frac{\partial u_{\mathbf{k}\sigma}^{\pm}}{\partial k_x}$ and using the fact that $\phi(\mathbf{r})$ (p_z -orbital) is an eigenstate of angular momentum, $L_z \phi(\mathbf{r}) = 0$, we can write

$$\begin{aligned} \frac{\partial H_{\mathbf{k}}}{\partial k_y} \frac{\partial u_{\mathbf{k}\sigma}^{\pm}}{\partial k_x} - \frac{\partial H_{\mathbf{k}}}{\partial k_x} \frac{\partial u_{\mathbf{k}\sigma}^{\pm}}{\partial k_y} &= \frac{\partial H_{\mathbf{k}}}{\partial k_y} \left[\pm \left(i \frac{\theta_x}{2} \frac{\Delta}{E} + \frac{s \varepsilon_x}{2t} \frac{\varepsilon}{E} \right) u_{\mathbf{k}\sigma}^{\pm} + \left(i \frac{\theta_x}{2} \frac{\varepsilon}{E} \mp \eta_x \pm \frac{i s \varepsilon}{2t} \theta_x - \frac{s \varepsilon_x}{2t} \frac{\Delta}{E} \right) u_{\mathbf{k}\sigma}^{\mp} \right] \\ &\quad - (x \leftrightarrow y) + O(s^2). \end{aligned} \quad (\text{B24})$$

Then we multiply $u_{\mathbf{k}\sigma}^{\pm*}$ and integrate the product. After some algebra, we obtain

$$\int u_{\mathbf{k}\sigma}^{\pm*} \left(\frac{\partial H_{\mathbf{k}}}{\partial k_{\mu}} \frac{\partial u_{\mathbf{k}\sigma}^{\pm}}{\partial k_{\nu}} - \frac{\partial H_{\mathbf{k}}}{\partial k_{\nu}} \frac{\partial u_{\mathbf{k}\sigma}^{\pm}}{\partial k_{\mu}} \right) d\mathbf{r} = i \frac{\Delta}{2E} (E_{\mu} \theta_{\nu} - E_{\nu} \theta_{\mu}) - 2i \varepsilon (\eta_{\mu} \theta_{\nu} - \eta_{\nu} \theta_{\mu}) + O(s^2). \quad (\text{B25})$$

Here, we have used the formulae (F5), and (F6). Combining Eqs. (B23) and (B25), we obtain (F7).

4. Derivation of (F8)

Similarly to the derivation of (F7), we calculate

$$\int u_{\mathbf{k}\sigma}^{\mp*} \left(\frac{\partial H_{\mathbf{k}}}{\partial k_{\mu}} \frac{\partial u_{\mathbf{k}\sigma}^{\pm}}{\partial k_{\mu}} + \frac{\partial H_{\mathbf{k}}}{\partial k_{\nu}} \frac{\partial u_{\mathbf{k}\sigma}^{\pm}}{\partial k_{\nu}} \right) d\mathbf{r}, \quad (\text{B26})$$

and

$$\int u_{\mathbf{k}\sigma}^{\mp*} \left(\frac{\partial H_{\mathbf{k}}}{\partial k_{\mu}} \frac{\partial u_{\mathbf{k}\sigma}^{\pm}}{\partial k_{\mu}} - \frac{\partial H_{\mathbf{k}}}{\partial k_{\nu}} \frac{\partial u_{\mathbf{k}\sigma}^{\pm}}{\partial k_{\nu}} \right) d\mathbf{r}. \quad (\text{B27})$$

First, we multiply $u_{\mathbf{k}\sigma}^{\mp*}$ to Eq.(B21) and integrate the product. Then we obtain

$$\int u_{\mathbf{k}\sigma}^{\mp*} \left(\frac{\partial H_{\mathbf{k}}}{\partial k_{\mu}} \frac{\partial u_{\mathbf{k}\sigma}^{\pm}}{\partial k_{\nu}} + \frac{\partial H_{\mathbf{k}}}{\partial k_{\nu}} \frac{\partial u_{\mathbf{k}\sigma}^{\pm}}{\partial k_{\mu}} \right) d\mathbf{r} = \pm E_{\mu} \int u_{\mathbf{k}\sigma}^{\mp*} \frac{\partial u_{\mathbf{k}\sigma}^{\pm}}{\partial k_{\nu}} d\mathbf{r} \pm E_{\nu} \int u_{\mathbf{k}\sigma}^{\mp*} \frac{\partial u_{\mathbf{k}\sigma}^{\pm}}{\partial k_{\mu}} d\mathbf{r} \pm 2E \int u_{\mathbf{k}\sigma}^{\mp*} \frac{\partial^2 u_{\mathbf{k}\sigma}^{\pm}}{\partial k_{\mu} \partial k_{\nu}} d\mathbf{r} \quad (\text{B28})$$

To calculate the last term, by differentiating (F2) by k_ν , we find a relation,

$$\begin{aligned} \int u_{\mathbf{k}\sigma}^{\pm*} \frac{\partial^2 u_{\mathbf{k}\sigma}^\mp}{\partial k_\mu \partial k_\nu} d\mathbf{r} &= - \int \frac{\partial u_{\mathbf{k}\sigma}^{\pm*}}{\partial k_\mu} \frac{\partial u_{\mathbf{k}\sigma}^\mp}{\partial k_\nu} d\mathbf{r} + \frac{\partial}{\partial k_\mu} \int u_{\mathbf{k}\sigma}^{\pm*} \frac{\partial u_{\mathbf{k}\sigma}^\mp}{\partial k_\nu} d\mathbf{r} \\ &= i \frac{\Delta}{2E} (\theta_\mu \eta_\nu + \theta_\nu \eta_\mu) + i \frac{\varepsilon}{2E} \theta_{\mu\nu} \pm \eta_{\mu\nu} - Y_{\mu\nu}^\pm + O(s^2), \end{aligned} \quad (\text{B29})$$

where we have used a relation Eq. (C1) or Eq. (C2). Substitution of this relation to Eq. (B28) leads to

$$\begin{aligned} \int u_{\mathbf{k}\sigma}^{\mp*} \left(\frac{\partial H_{\mathbf{k}}}{\partial k_\mu} \frac{\partial u_{\mathbf{k}\sigma}^\pm}{\partial k_\nu} + \frac{\partial H_{\mathbf{k}}}{\partial k_\nu} \frac{\partial u_{\mathbf{k}\sigma}^\pm}{\partial k_\mu} \right) d\mathbf{r} \\ = \pm \frac{i}{2} (\varepsilon_\mu \theta_\nu + \varepsilon_\nu \theta_\mu) - (E_\mu \eta_\nu + E_\nu \eta_\mu) \pm i \varepsilon \theta_{\mu\nu} \mp 2E Y_{\mu\nu}^\mp - 2E \eta_{\mu\nu} + O(s^2). \end{aligned} \quad (\text{B30})$$

On the other hand, using Eq. (B24), we obtain

$$\begin{aligned} \int u_{\mathbf{k}\sigma}^{\mp*} \left(\frac{\partial H_{\mathbf{k}}}{\partial k_\mu} \frac{\partial u_{\mathbf{k}\sigma}^\pm}{\partial k_\nu} - \frac{\partial H_{\mathbf{k}}}{\partial k_\nu} \frac{\partial u_{\mathbf{k}\sigma}^\pm}{\partial k_\mu} \right) d\mathbf{r} \\ = \pm \left(i \frac{\Delta \theta_\nu}{2E} + \frac{s \varepsilon \varepsilon_\nu}{2tE} \right) \int u_{\mathbf{k}\sigma}^{\mp*} \frac{\partial H_{\mathbf{k}}}{\partial k_\mu} u_{\mathbf{k}\sigma}^\pm d\mathbf{r} - (\mu \leftrightarrow \nu) \\ + \left(i \frac{\varepsilon \theta_\nu}{2E} \mp \eta_\nu \pm \frac{i s \varepsilon}{2t} \theta_\nu - \frac{s \Delta \varepsilon_\nu}{2tE} \right) \int u_{\mathbf{k}\sigma}^{\mp*} \frac{\partial H_{\mathbf{k}}}{\partial k_\mu} u_{\mathbf{k}\sigma}^\mp d\mathbf{r} - (\mu \leftrightarrow \nu) \\ = \mp \frac{i}{2} (\varepsilon_\mu \theta_\nu - \varepsilon_\nu \theta_\mu) - \frac{1}{2E} (\varepsilon_\mu \Delta_\nu - \varepsilon_\nu \Delta_\mu) + O(s^2), \end{aligned} \quad (\text{B31})$$

where we have used (F5), and (F6). Combining Eqs. (B30) and (B31), we obtain (F8).

Appendix C: Several relations between momentum derivatives

We find various relations between $E_\mu, \eta_\mu, \varepsilon_\mu, \Delta_\mu$, and θ_μ , which are used in various occasions. Using $\sin 2\eta = \varepsilon/E$ and $\cos 2\eta = \Delta/E$, we can see

$$\frac{\partial}{\partial k_\mu} \left(\frac{\varepsilon}{E} \right) = \frac{\partial}{\partial k_\mu} \sin 2\eta = 2\eta_\mu \cos 2\eta = \frac{2\Delta}{E} \eta_\mu. \quad (\text{C1})$$

By writing explicitly the left-hand side, we obtain

$$\Delta \eta_\mu + \frac{\varepsilon}{2E} E_\mu = \frac{\varepsilon_\mu}{2}. \quad (\text{C2})$$

Similarly, from the derivative of $\Delta/E = \cos 2\eta$, we have

$$-\varepsilon \eta_\mu + \frac{\Delta}{2E} E_\mu = \frac{\Delta_\mu}{2}, \quad (\text{C3})$$

which was used in the text Eq. (35). Furthermore, by making the k_ν -derivative of Eqs. (C2) and (C3), we obtain

$$E \eta_{\mu\nu} + E_\mu \eta_\nu + E_\nu \eta_\mu = \frac{1}{2E} (\Delta \varepsilon_{\mu\nu} - \varepsilon \Delta_{\mu\nu}). \quad (\text{C4})$$

and

$$E_{\mu\nu} - 4E \eta_\mu \eta_\nu = \frac{1}{E} (\varepsilon \varepsilon_{\mu\nu} + \Delta \Delta_{\mu\nu}). \quad (\text{C5})$$

In the previous paper, we obtained the following relationships:[24]

$$\begin{aligned} \varepsilon(\theta_x^2 + \theta_y^2) - \varepsilon_{xx} - \varepsilon_{yy} &= a^2 \varepsilon, \\ \varepsilon(\theta_{xx} + \theta_{yy}) + 2\varepsilon_x \theta_x + 2\varepsilon_y \theta_y &= 0, \end{aligned} \quad (\text{C6})$$

with a being the length between the nearest-neighbor carbons. These special relations hold since ε and θ are closely related to each other through $\gamma_{\mathbf{k}}$. Here we find additional relations.

Let us consider

$$\sum_{\mathbf{R}} (R_x^2 - R_y^2) e^{-i\mathbf{k} \cdot \mathbf{R}}, \quad (\text{C7})$$

where \mathbf{R} runs over the three vectors from a B site to its adjacent A sites. By using the explicit three vectors in Fig. 1, we can see that it is equal to

$$-ia \frac{\partial}{\partial k_y} \sum_{\mathbf{R}} e^{-i\mathbf{k} \cdot \mathbf{R}}. \quad (\text{C8})$$

Then, from the definitions of $\gamma_{\mathbf{k}}$ and θ , we can obtain the relationship:

$$\left(-\frac{\partial^2}{\partial k_x^2} + \frac{\partial^2}{\partial k_y^2} \right) |\gamma_{\mathbf{k}}| e^{i\theta} = -ia \frac{\partial}{\partial k_y} |\gamma_{\mathbf{k}}| e^{i\theta}. \quad (\text{C9})$$

By taking the real and imaginary part of both sides, we obtain

$$\begin{aligned} \varepsilon(\theta_x^2 - \theta_y^2) - \varepsilon_{xx} + \varepsilon_{yy} &= a \varepsilon \theta_y, \\ \varepsilon(\theta_{xx} - \theta_{yy}) + 2\varepsilon_x \theta_x - 2\varepsilon_y \theta_y &= a \varepsilon_y. \end{aligned} \quad (\text{C10})$$

From Eqs. (C6) and (C10), we can see

$$\begin{aligned}
\varepsilon_{xx} &= \varepsilon\theta_x^2 - \frac{a^2}{2}\varepsilon - \frac{a}{2}\varepsilon\theta_y, \\
\varepsilon_{yy} &= \varepsilon\theta_y^2 - \frac{a^2}{2}\varepsilon + \frac{a}{2}\varepsilon\theta_x, \\
\varepsilon\theta_{xx} &= -2\varepsilon_x\theta_x + \frac{a}{2}\varepsilon_y, \\
\varepsilon\theta_{yy} &= -2\varepsilon_y\theta_y - \frac{a}{2}\varepsilon_x,
\end{aligned} \tag{C11}$$

we obtain

$$\begin{aligned}
\varepsilon_{xy} &= \varepsilon\theta_x\theta_y - \frac{a}{2}\varepsilon\theta_x, \\
\varepsilon\theta_{xy} &= -\varepsilon_x\theta_y - \varepsilon_y\theta_x + \frac{a}{2}\varepsilon_x.
\end{aligned} \tag{C13}$$

Similarly by using

$$\sum_{\mathbf{R}} R_x R_y e^{-i\mathbf{k}\cdot\mathbf{R}} = -\frac{\partial^2}{\partial k_x \partial k_y} |\gamma_{\mathbf{k}}| e^{i\theta} = -i\frac{a}{2} \frac{\partial}{\partial k_x} |\gamma_{\mathbf{k}}| e^{i\theta}, \tag{C12}$$

Appendix D: Each contribution of χ

In the present case, the Landau-Peierls contribution simply becomes Eq. (38). Next, the l' -summation in χ_{inter} is carried out in Appendix E, and the result is given by

$$\begin{aligned}
\chi_{\text{inter}} &= \frac{e^2}{\hbar^2} \sum f(\pm E) \\
&\times \left[\left(\frac{\hbar^2}{16m} \pm \frac{\varepsilon^2}{4E} \langle y^2 \rangle \pm \frac{\hbar^2 s \varepsilon^2}{8m E t} \right) \theta_x^2 + \frac{\hbar^2}{4m} \left(\eta_x^2 \pm \frac{s\Delta}{Et} \eta_x \varepsilon_x \right) \pm E \langle y^2 \rangle \eta_x^2 \right. \\
&\pm \frac{\eta_x^2}{4E} (\varepsilon \varepsilon_{yy} + \Delta \Delta_{yy}) \mp \frac{\eta_x \eta_y}{4E} (\varepsilon \varepsilon_{xy} + \Delta \Delta_{xy}) \pm \frac{\theta_x^2}{16E} (\varepsilon \varepsilon_{yy} - \Delta \Delta_{yy}) \mp \frac{\theta_x \theta_y}{16E} (\varepsilon \varepsilon_{xy} - \Delta \Delta_{xy}) \\
&\left. \pm \frac{\theta_x^2}{4E} (\Delta \varepsilon_y \eta_y - E^2 \eta_y^2) \mp \frac{\theta_x \theta_y}{4E} (\Delta \varepsilon_x \eta_y - E^2 \eta_x \eta_y) \mp \frac{\varepsilon \Delta}{4E} (\eta_x \theta_x \theta_{yy} - \eta_x \theta_y \theta_{xy}) \right] + (x \leftrightarrow y) + O(s^2). \tag{D1}
\end{aligned}$$

For χ_{FS} , we multiply the Hermitian conjugate of Eq. (B24) by $\frac{\partial u_{\mathbf{k}\sigma}^\pm}{\partial k_y}$ and integrate the product. Then, with the help of (F7) and (F8), we obtain

$$\begin{aligned}
\chi_{\text{FS}} &= \frac{e^2}{2\hbar^2} \sum_{\pm k\sigma} f'(\pm E) \left[\frac{\hbar^2 s \varepsilon}{2m 2tE} \varepsilon_x E_x + \frac{\varepsilon^2 E_x}{4E} (\theta_y \theta_{xy} - \theta_x \theta_{yy}) + \frac{\Delta E_x}{4E} (\Delta_x \theta_y^2 - \Delta_y \theta_x \theta_y) \right. \\
&+ \frac{E_x}{2E} \{ \eta_y (\Delta \varepsilon_{xy} - \varepsilon \Delta_{xy}) - \eta_x (\Delta \varepsilon_{yy} - \varepsilon \Delta_{yy}) \} + E_x^2 \left(\langle y^2 \rangle + \frac{1}{4} \theta_y^2 \right) - \frac{1}{4} E_x E_y \theta_x \theta_y + (x \leftrightarrow y) \left. \right] \\
&+ \frac{e^2}{2\hbar^2} \sum_{\pm k\sigma} f'(\pm E) \frac{\hbar^2 \Delta}{m 2E} \sigma (E_x \theta_y - E_y \theta_x) + O(s^2), \tag{D2}
\end{aligned}$$

where we have used the relation in Eqs. (C3) and (C4). The last term in Eq. (D2) comes from the contribution of the Zeeman term. We find that it is convenient to make partial integrations in the last three terms, which will be

included in χ_1, χ_2 , and χ_{OZ} in the main text. With the partial integrations, we obtain

$$\begin{aligned} \chi_{\text{FS}} = & \frac{e^2}{2\hbar^2} \sum_{\pm, \mathbf{k}, \sigma} f'(\pm E) \left[\frac{\hbar^2}{2m} \frac{s\varepsilon}{2tE} \varepsilon_x E_x + \frac{\varepsilon^2 E_x}{4E} (\theta_y \theta_{xy} - \theta_x \theta_{yy}) + \frac{\Delta E_x}{4E} (\Delta_x \theta_y^2 - \Delta_y \theta_x \theta_y) \right. \\ & \left. + \frac{E_x}{2E} \{ \eta_y (\Delta \varepsilon_{xy} - \varepsilon \Delta_{xy}) - \eta_x (\Delta \varepsilon_{yy} - \varepsilon \Delta_{yy}) \} + (x \leftrightarrow y) \right] \\ & - \frac{e^2}{2\hbar^2} \sum_{\pm, \mathbf{k}, \sigma} f(\pm E) \left[\pm E_{xx} \left(\langle y^2 \rangle + \frac{1}{4} \theta_y^2 \right) \mp \frac{1}{4} E_{xy} \theta_x \theta_y \mp \frac{1}{4} (E_x \theta_x \theta_{yy} - E_x \theta_y \theta_{xy}) + (x \leftrightarrow y) \right] \\ & - \frac{e^2}{2\hbar^2} \sum_{\pm, \mathbf{k}, \sigma} f(\pm E) \frac{\hbar^2}{m} \sigma \left\{ \left(\frac{\Delta_x}{2E} - \frac{\Delta E_x}{2E^2} \right) \theta_y - \left(\frac{\Delta_y}{2E} - \frac{\Delta E_y}{2E^2} \right) \theta_x \right\} + O(s^2), \end{aligned} \quad (\text{D3})$$

$\chi_{\text{FS-P}}$ is directly obtained by substituting $M_{\pm\pm\sigma}$ as

$$\chi_{\text{FS-P}} = - \sum_{\pm, \mathbf{k}, \sigma} f'(\pm E) \left[\frac{e^2}{4\hbar^2} (\Delta_x \theta_y - \Delta_y \theta_x)^2 + \frac{e^2}{2m} \sigma (\Delta_x \theta_y - \Delta_y \theta_x) + \frac{e^2 \hbar^2}{4m^2} \sigma^2 \right] + O(s^2). \quad (\text{D4})$$

Using the integration formulae (F3) in Appendix B, we obtain χ_{occ1} as

$$\begin{aligned} \chi_{\text{occ1}} = & - \frac{e^2}{4\hbar^2} \sum_{\pm, \mathbf{k}, \sigma} f(\pm E) \left[\pm E_{xy} \left(\frac{1}{4} \theta_x \theta_y + \eta_x \eta_y \right) + \left(\frac{\hbar^2}{m} \mp E_{xx} \right) \left(\langle y^2 \rangle + \frac{1}{4} \theta_y^2 + \eta_y^2 \right) \right. \\ & \left. \mp \frac{\hbar^2}{m} \frac{\varepsilon}{E} \text{Re} X_{yy} \right] + (x \leftrightarrow y) + O(s^2), \end{aligned} \quad (\text{D5})$$

Finally χ_{occ2} becomes

$$\chi_{\text{occ2}} = \frac{e^2}{\hbar^2} \sum_{\pm, \mathbf{k}, \sigma} f(\pm E) \left[\mp \frac{\varepsilon}{2E} \{ \theta_x^2 \Delta_y \eta_y - \theta_x \theta_y \Delta_x \eta_y + (x \leftrightarrow y) \} \pm \frac{\hbar^2}{2m} \frac{\varepsilon}{E} \sigma (\theta_x \eta_y - \theta_y \eta_x) \right] + O(s^2). \quad (\text{D6})$$

In the total of these contributions, some terms cancel with each other. In the zeroth order of s (s^0), there are terms proportional to $\frac{\hbar^2}{m} \langle y^2 \rangle$ and $\frac{\hbar^2}{m} \theta_x^2$ in χ_{occ1} and χ_{inter} . However, the latter cancels with each other and only the former appearing in χ_{occ1} contributes to the total susceptibility in the zeroth order. In the previous paper,[24] we call this contribution as ‘‘inraband atomic diamagnetism’’, which is shown as χ_{atomic} in Eq. (41).

Collecting the contributions proportional to \hbar^2/m and $\langle y^2 \rangle$ and using integration by parts for terms in χ_{FS} , we obtain

$$\begin{aligned} \chi_2 = & \frac{e^2}{\hbar^2} \sum_{\pm, \mathbf{k}, \sigma} f(\pm E) \left[\mp \frac{\langle y^2 \rangle}{4E} (\varepsilon \varepsilon_{xx} + \Delta \Delta_{xx} - \varepsilon^2 \theta_x^2) \right. \\ & \left. \mp \frac{\hbar^2}{4m} \left(\frac{s\varepsilon}{2Et} (\varepsilon_{xx} - \varepsilon \theta_x^2) - \frac{\varepsilon}{E} \text{Re} X_{yy} \right) \right] + (x \leftrightarrow y) + O(s^2). \end{aligned} \quad (\text{D7})$$

where we have used the relations of Eqs. (C1) and (C5). Finally when we use the relation Eq. (C11), we obtain Eq. (43). The last term in $\chi_{\text{FS-P}}$ is the usual Pauli paramagnetism, Eq. (39). The orbital-Zeeman (OZ) cross-terms are characterized by the presence of σ and they appear in χ_{FS} , $\chi_{\text{FS-P}}$, and χ_{occ2} . Their total becomes

$$\begin{aligned} \chi_{\text{OZ}} = & \frac{e^2}{\hbar^2} \sum_{\pm, \mathbf{k}, \sigma} f'(\pm E) \frac{\hbar^2}{m} \sigma \left[(\varepsilon (\eta_x \theta_y - \eta_y \theta_x) - \frac{\Delta}{4E} (E_x \theta_y - E_y \theta_x)) \right. \\ & \left. + \frac{e^2}{\hbar^2} \sum_{\pm, \mathbf{k}, \sigma} f(\pm E) \left[\pm \frac{\hbar^2}{2m} \sigma \frac{\varepsilon}{E} (\theta_x \eta_y - \theta_y \eta_x) \right] + O(s^2), \end{aligned} \quad (\text{D8})$$

where we have used Eq. (C3) for Δ_x and Δ_y . Then using the integration by parts in the second term and using Eq. (C3) again, we obtain χ_{OZ} in Eq. (40). The other terms lead to Eq. (42).

Appendix E: l' summation in χ_{inter}

To carry out the summation in χ_{inter} Eq. (25), we first consider the case of $l' = \mp$. From (F2) and (F8), we have

$$M_{\pm\mp\sigma}^z = \mp \frac{e}{2\hbar} \Delta (\eta_x \theta_y - \eta_y \theta_x), \quad (\text{E1})$$

where we have used a relation Eq. (C3). Then, we have

$$-2 \sum_{\pm, \mathbf{k}, \sigma} \frac{f(\pm E)}{(\pm E) - (\mp E)} |M_{\pm\mp\sigma}^z|^2 = -\frac{e^2}{2\hbar^2} \sum_{\pm, \mathbf{k}, \sigma} f(\pm E) \left[\pm \frac{\Delta^2}{2E} (\eta_x \theta_y - \eta_y \theta_x)^2 \right]. \quad (\text{E2})$$

Next, we consider the case of $l' \neq \pm, \mp$. In this case, using Eq. (B24) we can rewrite $M_{\pm l'\sigma}^z$ as

$$M_{\pm l'\sigma}^z = -\frac{ie}{2\hbar} \left[A_x (\pm E - E_{l'}) \int \frac{\partial u_{\mathbf{k}\sigma}^{\pm*}}{\partial k_y} u_{l'\mathbf{k}\sigma} d\mathbf{r} + B_x (\mp E - E_{l'}) \int \frac{\partial u_{\mathbf{k}\sigma}^{\mp*}}{\partial k_y} u_{l'\mathbf{k}\sigma} d\mathbf{r} \right. \\ \left. \pm E_y \int \frac{\partial u_{\mathbf{k}\sigma}^{\pm*}}{\partial k_x} u_{l'\mathbf{k}\sigma} d\mathbf{r} \right] - (x \leftrightarrow y), \quad (\text{E3})$$

where

$$A_\mu = \mp i \frac{\Delta}{2E} \theta_\mu \pm \frac{s}{2t} \frac{\varepsilon}{E} \varepsilon_\mu \\ B_\mu = -i \frac{\varepsilon}{2E} \theta_\mu \mp \eta_\mu \mp i \frac{s\varepsilon}{2t} \theta_\mu - \frac{s}{2t} \frac{\Delta}{E} \varepsilon_\mu, \quad (\text{E4})$$

for $\mu = x, y$. Then, $M_{\pm l'\sigma}^z$ can be rewritten as

$$M_{\pm l'\sigma}^z = (M_1^{xy} + M_2^{xy}) - (x \leftrightarrow y), \quad (\text{E5})$$

with

$$M_1^{\mu\nu} \equiv -\frac{ie}{2\hbar} \{A_\mu (\pm E - E_{l'}) \mp E_\mu\} \int \frac{\partial u_{\mathbf{k}\sigma}^{\pm*}}{\partial k_\nu} u_{l'\mathbf{k}\sigma} d\mathbf{r} \\ M_2^{\mu\nu} \equiv -\frac{ie}{2\hbar} \{B_\mu (\pm E - E_{l'}) \mp 2EB_\mu\} \int \frac{\partial u_{\mathbf{k}\sigma}^{\mp*}}{\partial k_\nu} u_{l'\mathbf{k}\sigma} d\mathbf{r}. \quad (\text{E6})$$

Using these abbreviations, $|M_{\pm l'\sigma}^z|^2$ becomes

$$|M_{\pm l'\sigma}^z|^2 = |M_1^{xy}|^2 + |M_2^{xy}|^2 + (M_1^{xy} M_2^{xy*} + \text{c.c.}) - M_1^{xy} M_1^{yx*} - M_2^{xy} M_2^{yx*} - (M_1^{xy} M_2^{yx*} + \text{c.c.}) \\ + (x \leftrightarrow y). \quad (\text{E7})$$

Thus, we need to calculate the six types of matrix elements. In these calculations, we can write the l' summation in a form,

$$\sum_{l' \neq \pm, \mp} \frac{(\pm E - E_{l'})^n}{\pm E - E_{l'}} \int X^* u_{l'\mathbf{k}\sigma} d\mathbf{r} \int u_{l'\mathbf{k}\sigma}^* Y d\mathbf{r}, \quad (\text{E8})$$

with $n = 0, 1$, and 2 , and

$$X, Y = \frac{\partial u_{\mathbf{k}\sigma}^{\pm}}{\partial k_\mu}, \frac{\partial u_{\mathbf{k}\sigma}^{\mp}}{\partial k_\nu}, \quad \text{etc.} \quad (\text{E9})$$

We can carry out these l' summation in the following ways:

(a) $n = 0$ case:

The denominator $\pm E - E_{l'}$ is in the zero-th order with respect to s , and the numerator is in the second order of s because the prefactors E_μ and EB_μ are both in the order of $O(s)$. Therefore, we can neglect this contribution of $n = 0$ in the calculation in the order of $O(s)$.

(b) $n = 1$ case:

Using the completeness condition, $\sum_{l'} u_{l'}(\mathbf{r})u_{l'}^*(\mathbf{r}') = \delta(\mathbf{r} - \mathbf{r}')$, we obtain

$$\sum_{l' \neq \pm, \mp} \int X^* u_{l'} d\mathbf{r} \int u_{l'}^* Y d\mathbf{r} = \int X^* Y d\mathbf{r} - \int X^* u_{\mathbf{k}\sigma}^{\pm} d\mathbf{r} \int u_{\mathbf{k}\sigma}^{\pm*} Y d\mathbf{r} - \int X^* u_{\mathbf{k}\sigma}^{\mp} d\mathbf{r} \int u_{\mathbf{k}\sigma}^{\mp*} Y d\mathbf{r}. \quad (\text{E10})$$

(c) $n = 2$ case:

Similarly, using the completeness condition,

$$\begin{aligned} \sum_{l' \neq \pm, \mp} \frac{(\pm E - E_{l'})^2}{\pm E - E_{l'}} \int X^* u_{l'} d\mathbf{r} \int u_{l'}^* Y d\mathbf{r} &= \sum_{l' \neq \pm, \mp} \int X^* (\pm E - H_{\mathbf{k}\sigma}) u_{l'} d\mathbf{r} \int u_{l'}^* Y d\mathbf{r} \\ &= \int X^* (\pm E - H_{\mathbf{k}\sigma}) Y d\mathbf{r} \mp 2E \int X^* u_{\mathbf{k}\sigma}^{\mp} d\mathbf{r} \int u_{\mathbf{k}\sigma}^{\mp*} Y d\mathbf{r}. \end{aligned} \quad (\text{E11})$$

Using the formulae (F1)-(F8), (B18), (E10), and (E11), we can carry out the summation of all the combinations as follows,

$$\sum_{l' \neq \pm, \mp} \frac{|M_1^{xy}|^2}{\pm E - E_{l'}} = \frac{e^2}{4\hbar^2} \left[|A_x|^2 \left\{ -\frac{\hbar^2}{2m} \pm \frac{1}{2} E_{yy} \mp \frac{\varepsilon^2}{2E} \theta_y^2 \mp 2E\eta_y^2 \right\} \mp 2E_x \text{Re}[A_x] \langle y^2 \rangle + O(s^2) \right], \quad (\text{E12})$$

$$\sum_{l' \neq \pm, \mp} \frac{|M_2^{xy}|^2}{\pm E - E_{l'}} = \frac{e^2}{4\hbar^2} \left[|B_x|^2 \left\{ -\frac{\hbar^2}{2m} \mp \frac{1}{2} E_{yy} \pm \frac{\varepsilon^2}{2E} \theta_y^2 \pm 2E\eta_y^2 \mp 2E \langle y^2 \rangle \right\} + O(s^2) \right], \quad (\text{E13})$$

$$\sum_{l' \neq \pm, \mp} \frac{M_1^{xy} M_2^{xy*}}{\pm E - E_{l'}} = \frac{e^2}{4\hbar^2} \left[A_x B_x^* \left\{ \mp \frac{i}{2} (2\varepsilon_y \theta_y + \varepsilon \theta_{yy}) - \frac{1}{2E} (\Delta\varepsilon_{yy} - \varepsilon \Delta_{yy} - \varepsilon \Delta \theta_y^2) \right\} + O(s^2) \right], \quad (\text{E14})$$

$$\sum_{l' \neq \pm, \mp} \frac{M_1^{xy} M_1^{yx*}}{\pm E - E_{l'}} = \frac{e^2}{4\hbar^2} \left[\pm A_x A_y^* \left(\frac{1}{2} E_{xy} - \frac{\varepsilon^2}{2E} \theta_x \theta_y - 2E\eta_x \eta_y \right) + O(s^2) \right], \quad (\text{E15})$$

$$\sum_{l' \neq \pm, \mp} \frac{M_2^{xy} M_2^{yx*}}{\pm E - E_{l'}} = \frac{e^2}{4\hbar^2} \left[\mp B_x B_y^* \left(\frac{1}{2} E_{xy} - \frac{\varepsilon^2}{2E} \theta_x \theta_y - 2E\eta_x \eta_y \right) + O(s^2) \right], \quad (\text{E16})$$

$$\sum_{l' \neq \pm, \mp} \frac{M_1^{xy} M_2^{yx*}}{\pm E - E_{l'}} = \frac{e^2}{4\hbar^2} \left[A_x B_y^* \left\{ \mp \frac{i}{2} (\varepsilon_x \theta_y + \varepsilon_y \theta_x + \varepsilon \theta_{xy}) - \frac{1}{2E} (\Delta\varepsilon_{xy} - \varepsilon \Delta_{xy} - \varepsilon \Delta \theta_x \theta_y) \right\} + O(s^2) \right]. \quad (\text{E17})$$

Here we have used the relation in Eq. (C4). Then, substituting A_μ and B_μ , and keeping the terms up to the order of $O(s)$, we obtain Eq. (D1).

-
- [1] F. D. M. Haldane, Model for a quantum hall effect without landau levels: Condensed-matter realization of the "parity anomaly", Phys. Rev. Lett. **61**, 2015 (1988).
- [2] C. L. Kane and E. J. Mele, Quantum spin hall effect in graphene, Phys. Rev. Lett. **95**, 226801 (2005).
- [3] C. L. Kane and E. J. Mele, Z_2 topological order and the quantum spin hall effect, Phys. Rev. Lett. **95**, 146802 (2005).
- [4] B. A. Bernevig and S.-C. Zhang, Quantum spin hall effect, Phys. Rev. Lett. **96**, 106802 (2006).
- [5] B. A. Bernevig, T. L. Hughes, and S.-C. Zhang, Quantum spin hall effect and topological phase transition in hgte quantum wells, Science **314**, 1757 (2006), <https://www.science.org/doi/pdf/10.1126/science.1133734>.
- [6] M.-F. Yang and M.-C. Chang, Středa-like formula in the spin hall effect, Phys. Rev. B **73**, 073304 (2006).
- [7] S. Murakami, Quantum spin hall effect and enhanced magnetic response by spin-orbit coupling, Phys. Rev. Lett. **97**, 236805 (2006).
- [8] M. König, S. Wiedmann, C. Brüne, A. Roth, H. Buhmann, L. W. Molenkamp, X.-L. Qi, and S.-C. Zhang, Quantum spin hall insulator state in hgte quantum wells, Science **318**, 766 (2007), <https://www.science.org/doi/pdf/10.1126/science.1148047>.
- [9] A. Roth, C. Brüne, H. Buhmann, L. W. Molenkamp, J. Maciejko, X.-L. Qi, and S.-C. Zhang, Nonlocal transport in the quantum spin hall state, Science **325**, 294 (2009), <https://www.science.org/doi/pdf/10.1126/science.1174736>.
- [10] C. Brüne, A. Roth, H. Buhmann, E. M. Hankiewicz, L. W. Molenkamp, J. Maciejko, X.-L. Qi, and S.-C. Zhang, Spin polarization of the quantum spin hall edge

- states, *Nature Physics* **8**, 485 (2012).
- [11] I. Knez, R.-R. Du, and G. Sullivan, Evidence for helical edge modes in inverted InAs/GaSb quantum wells, *Phys. Rev. Lett.* **107**, 136603 (2011).
- [12] I. Knez, R.-R. Du, and G. Sullivan, Andreev reflection of helical edge modes in InAs/GaSb quantum spin hall insulator, *Phys. Rev. Lett.* **109**, 186603 (2012).
- [13] L. Fu and C. L. Kane, Topological insulators with inversion symmetry, *Phys. Rev. B* **76**, 045302 (2007).
- [14] D. Hsieh, D. Qian, L. Wray, Y. Xia, Y. S. Hor, R. J. Cava, and M. Z. Hasan, A topological dirac insulator in a quantum spin hall phase, *Nature* **452**, 970 (2008).
- [15] R. Nakai and K. Nomura, Crossed responses of spin and orbital magnetism in topological insulators, *Phys. Rev. B* **93**, 214434 (2016).
- [16] Y. Tserkovnyak, D. A. Pesin, and D. Loss, Spin and orbital magnetic response on the surface of a topological insulator, *Phys. Rev. B* **91**, 041121 (2015).
- [17] M. Koshino and I. F. Hizbullah, Magnetic susceptibility in three-dimensional nodal semimetals, *Phys. Rev. B* **93**, 045201 (2016).
- [18] H. Suzuura and T. Ando, Theory of magnetic response in two-dimensional giant rashba system, *Phys. Rev. B* **94**, 085303 (2016).
- [19] Y. Ominato, S. Tatsumi, and K. Nomura, Spin-orbit crossed susceptibility in topological dirac semimetals, *Phys. Rev. B* **99**, 085205 (2019).
- [20] T. Aftab and K. Sabeeh, Anisotropic magnetic response of weyl semimetals in a topological insulator multilayer, *Journal of Applied Physics* **127**, 163905 (2020), <https://doi.org/10.1063/1.5142216>.
- [21] S. Ozaki and M. Ogata, Universal quantization of the magnetic susceptibility jump at a topological phase transition, *Phys. Rev. Research* **3**, 013058 (2021).
- [22] M. Ogata and H. Fukuyama, Orbital magnetism of bloch electrons i. general formula, *Journal of the Physical Society of Japan* **84**, 124708 (2015), <https://doi.org/10.7566/JPSJ.84.124708>.
- [23] M. Ogata, Orbital magnetism of bloch electrons: ii. application to single-band models and corrections to landau-peierls susceptibility, *Journal of the Physical Society of Japan* **85**, 064709 (2016), <https://doi.org/10.7566/JPSJ.85.064709>.
- [24] M. Ogata, Orbital magnetism of bloch electrons: lii. application to graphene, *Journal of the Physical Society of Japan* **85**, 104708 (2016), <https://doi.org/10.7566/JPSJ.85.104708>.
- [25] P. Löwdin, On the non-orthogonality problem connected with the use of atomic wave functions in the theory of molecules and crystals, *The Journal of Chemical Physics* **18**, 365 (1950), <https://doi.org/10.1063/1.1747632>.
- [26] H. Matsuura and M. Ogata, Theory of orbital susceptibility in the tight-binding model: Corrections to the peierls phase, *Journal of the Physical Society of Japan* **85**, 074709 (2016), <https://doi.org/10.7566/JPSJ.85.074709>.
- [27] L. Landau, Diamagnetismus der metalle, *Zeitschrift für Physik* **64**, 629 (1930).
- [28] R. Peierls, Zur theorie des diamagnetismus von leitungslektronen, *Zeitschrift für Physik* **80**, 763 (1933).
- [29] H. Fukuyama and R. Kubo, Interband effects on magnetic susceptibility. ii. diamagnetism of bismuth, *Journal of the Physical Society of Japan* **28**, 570 (1970), <https://doi.org/10.1143/JPSJ.28.570>.
- [30] J. Hebborn and E. Sondheimer, The diamagnetism of conduction electrons in metals, *Journal of Physics and Chemistry of Solids* **13**, 105 (1960).
- [31] E. I. Blount, Bloch electrons in a magnetic field, *Phys. Rev.* **126**, 1636 (1962).
- [32] J. E. Hebborn, J. M. Luttinger, E. H. Sondheimer, and P. J. Stiles, *J. Phys. Chem. Solids* **25**, 741 (1964).
- [33] H. Fukuyama, Theory of Orbital Magnetism of Bloch Electrons: Coulomb Interactions, *Progress of Theoretical Physics* **45**, 704 (1971), <https://academic.oup.com/ptp/article-pdf/45/3/704/5249600/45-3-7>
- [34] G. Gómez-Santos and T. Stauber, Measurable lattice effects on the charge and magnetic response in graphene, *Phys. Rev. Lett.* **106**, 045504 (2011).
- [35] A. Raoux, F. Piéchon, J.-N. Fuchs, and G. Montambaux, Orbital magnetism in coupled-bands models, *Phys. Rev. B* **91**, 085120 (2015).
- [36] M. Ogata, Theory of magnetization in bloch electron systems, *Journal of the Physical Society of Japan* **86**, 044713 (2017), <https://doi.org/10.7566/JPSJ.86.044713>.
- [37] M. Ezawa, A topological insulator and helical zero mode in silicene under an inhomogeneous electric field, *New J. Phys.* **14**, 033003 (2012).
- [38] M. Ezawa, Topological phase transition and electrically tunable diamagnetism in silicene, *The European Physical Journal B* **85**, 363 (2012).
- [39] G. G. Guzmán-Verri and L. C. Lew Yan Voon, Electronic structure of silicon-based nanostructures, *Phys. Rev. B* **76**, 075131 (2007).
- [40] C.-C. Liu, H. Jiang, and Y. Yao, Low-energy effective hamiltonian involving spin-orbit coupling in silicene and two-dimensional germanium and tin, *Phys. Rev. B* **84**, 195430 (2011).
- [41] C.-C. Liu, W. Feng, and Y. Yao, Quantum spin hall effect in silicene and two-dimensional germanium, *Phys. Rev. Lett.* **107**, 076802 (2011).
- [42] L. M. Roth, B. Lax, and S. Zwerdling, Theory of optical magneto-absorption effects in semiconductors, *Phys. Rev.* **114**, 90 (1959).
- [43] C.-X. Liu, X.-L. Qi, H. Zhang, X. Dai, Z. Fang, and S.-C. Zhang, Model hamiltonian for topological insulators, *Phys. Rev. B* **82**, 045122 (2010).
- [44] J. C. Slater, Atomic shielding constants, *Phys. Rev.* **36**, 57 (1930).
- [45] S. Blundell, *Magnetism in Condensed Matter* (Oxford University Press).
- [46] D. N. Sheng, Z. Y. Weng, L. Sheng, and F. D. M. Haldane, Quantum spin-hall effect and topologically invariant chern numbers, *Phys. Rev. Lett.* **97**, 036808 (2006).
- [47] D. Xiao, M.-C. Chang, and Q. Niu, Berry phase effects on electronic properties, *Rev. Mod. Phys.* **82**, 1959 (2010).
- [48] T. THONHAUSER, Theory of orbital magnetization in solids, *International Journal of Modern Physics B* **25**, 1429 (2011), <https://doi.org/10.1142/S0217979211058912>.
- [49] G. Sundaram and Q. Niu, Wave-packet dynamics in slowly perturbed crystals: Gradient corrections and berry-phase effects, *Phys. Rev. B* **59**, 14915 (1999).
- [50] D. Xiao, J. Shi, and Q. Niu, Berry phase correction to electron density of states in solids, *Phys. Rev. Lett.* **95**, 137204 (2005).
- [51] T. Thonhauser, D. Ceresoli, D. Vanderbilt, and

- R. Resta, Orbital magnetization in periodic insulators, Phys. Rev. Lett. **95**, 137205 (2005).
- [52] D. Ceresoli, T. Thonhauser, D. Vanderbilt, and R. Resta, Orbital magnetization in crystalline solids: Multi-band insulators, chern insulators, and metals, Phys. Rev. B **74**, 024408 (2006).
- [53] J. Shi, G. Vignale, D. Xiao, and Q. Niu, Quantum theory of orbital magnetization and its generalization to interacting systems, Phys. Rev. Lett. **99**, 197202 (2007).